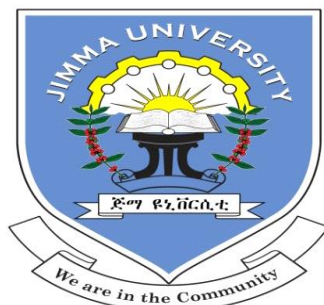


JIMMA UNIVERSITY
SCHOOL OF GRADUATE STUDIES
COLLEGE OF NATURAL SCIENCE
DEPARTMENT OF CHEMISTRY



MSC THESIS ON:

**GREEN SYNTHESIS OF COPPER OXIDE AND COBALT DOPED
COPPER OXIDE NANOMATERIALS USING *Kalanchoe petitiانا*
(ENDAHULA) LEAF EXTRACTS AND EVALUATION OF ITS
ANTIMICROBIAL ACTIVITY**

BY: ESAYAS BUDARE

ADVISOR: GUTA GONFA (Ph.D.)

CO- ADVISOR: AHMED AWOL (Ass.prof)

APRIL, 2022
JIMMA, ETHIOPIA

**GREEN SYNTHESIS OF COPPER OXIDE AND COBALT DOPED
COPPER OXIDE NANOMATERIALS USING *Kalanchoe petiti*
(ENDAHULA) LEAF EXTRACTS AND EVALUATION OF ITS
ANTIMICROBIAL ACTIVITY**

A THESIS SUBMITTED TO JIMMA UNIVERSITY, SCHOOL OF
GRADUATE STUDIES, IN PARTIAL FULFILMENT OF THE
REQUIREMENTS FOR DEGREE OF MASTER OF SCIENCE IN
CHEMISTRY.

BY: ESAYAS BUDARE

ADVISOR: GUTA GONFA (Ph.D.)

CO- ADVISOR: AHMED AWEL (Ass. prof)

**APRIL, 2022
JIMMA, ETHIOPIA**

DECLARATION

I, the undersigned, declare that this thesis work is my original work, and to the best of my knowledge, it has never been submitted to any university, college, or institution anywhere for the award of any academic degree, diploma, or certificate and I affirm that I have cited and referenced all sources used in this document.

Name: Esayas Budare

Signature: _____

This thesis has been submitted for examination with my approval as University

Advisor and Co-advisor

Name of advisor: Guta Gonfa (PhD)

Signature: _____

Name of Co-advisor: Ahmed Awel (Ass.prof)

Signature: _____

Green synthesis of copper oxide and cobalt-doped copper oxide nanoparticles using *Kalanchoe petitiiana* (Endahula) leaf extracts and evaluation of its antimicrobial activity.

By: Esayas Budare

A Thesis Submitted to Jimma University, School of Graduate Studies in Partial Fulfilment of the Requirements for the Degree of Masters of Science in Chemistry.

APPROVED BY BOARD OF EXAMINERS

Principal Advisor	Signature	Date
_____	_____	_____
Co-advisor		
_____	_____	_____
Internal examiner		
_____	_____	_____
External examiner		
_____	_____	_____
Chair person		
_____	_____	_____
Head of the department		
_____	_____	_____

April 2022
Jimma, Ethiopia

DEDICATION

This work is dedicated to "THE ALMIGHTY GOD", who in his infinite mercy granted me the wisdom and understanding to carry out this work from start to finish.

ACKNOWLEDGMENT

First and foremost let me praise and honor the Almighty God bestowing up on my health, strength, patience, and protection to realize my hope.

Secondly, I would like to express my deepest gratitude to my advisor Dr. Guta Gonfa for his unreserved cooperation, constructive suggestions, supervision, appreciable encouragement, and fatherly consultancy and also my co-advisor Mr. Ahmed Awel for examples of intellectual interest and integrity and also sets a tone of free thinking and enormous scientific excitement in my mind.

I would like to express my thanks to the Department of Chemistry, Jimma University, for providing laboratory facilities and materials throughout my study.

Special thanks to laboratory technical assistance in analyzing samples by Fourier transform infrared (FTIR) spectrometer and UV-Vis analysis and also thanks to laboratory assistance in Jimma university institute of technology, department of material science, technical assistance in analyzing samples by X-ray Powder Diffraction (XRD) spectrometer and also thanks to Adama science and technology university in analyzing samples by SEM.

My acknowledgment is also extended to the Ministry of Education for allowing me to join this postgraduate program and for sponsorship of my study.

Finally, my cheerful thanks go to my parents and all the family members who give me moral and material support during my study.

TABLE OF CONTENTS	PAGE
ACKNOWLEDGMENT.....	I
TABLE OF CONTENTS.....	II
LIST OF FIGURES.....	VI
LIST OF TABLES.....	VII
LIST OF ABBREVIATIONS.....	VIII
ABSTRACT.....	VIII
1.INTRODUCTION.....	1
1.1.Background of the studies.....	1
1.1.3.Statement of the problem.....	3
1.2. Objectives.....	4
1.2.1. General objective.....	4
1.2.2. Specific objectives.....	4
1.3.Significance of the study.....	4
2. LITERATURE REVIEW.....	6
2.1. Overview of nanoparticles, nanotechnology, and nanoscience.....	6
2.2. Need for green synthesis.....	7
2.3. About Kalanchoe petitiiana.....	8
2.4. Pharmacological medicinal use of Kalanchoe petitiiana.....	8
2.5. CuO and Co-doped Copper oxide nanomaterials.....	8
2.6. Biomedical applications of copper oxide nanomaterials.....	9

2.6.1. Antibacterial activity.....	10
2.6.2. Antifungal activity.....	10
2.7. Techniques of synthesis of CuO and Co-doped CuO nanomaterials.....	10
2.7.1. Top down approach.....	11
2.7.2. Bottom-up approaches.....	11
2.8. Biosynthesis of CuO and Co-doped CuO nanomaterials.....	12
2.9. Factors affecting biosynthesis of nanoparticles.....	14
2.9.1. Concentration of Plant Extracts.....	14
2.9.2. Precursor Used.....	14
2.9.3. pH measurements.....	15
2.10. Characterization technique.....	15
2.10.1. UV-Visible absorption techniques.....	15
2.10.2 X-ray diffraction (XRD) techniques.....	15
2.10.3. Fourier transform infrared (FTIR) spectroscopy	16
2.10.4. Electrochemical Studies.....	16
2.11. Applications of nanoparticles to human health and environments.....	16
3.MATERIAL AND METHODS.....	17
3.1 study area.....	17
3.1.2. Chemicals and reagents.....	17
3.1.3. Instruments.....	17
3.2. Sample collection and preparation of plant extract.....	17

3.3. Qualitative Phytochemical Screening.....	18
3.4 Optimization of CuO NMS.....	19
3.5. Biosynthesis of CuO and Co-doped CuO nanomaterials.....	19
3.6. Characterization of CuO and Co-doped CuO nanomaterials.....	21
3.6.1. UV-Visible absorption spectroscopy analysis.....	21
3.6.2. X-ray diffraction (XRD) analysis.....	21
3.6.3. Fourier Transform Infrared [FTIR] spectroscopy analysis.....	21
3.6.4. Electrochemical analysis.....	22
3.6.4. Antimicrobial Activity analysis.....	22
3.6.5. Preparation of inoculums.....	22
3.6.6. Preparation of test solutions.....	23
3.6.7. Disc diffusion method for antifungal activity.....	23
4. RESULT AND DISCUSSION.....	24
4.1. Photochemical testing of the plant extracts.....	24
4.3. Optimization of CuO NMs.....	25
4.3.1. Optimization pH effects of CuO NMs.....	25
4.3.2. Optimization of precursor Concentration of Cu (NO ₃) ₂ .3H ₂ O.....	26
4.3.3. Optimization of Plant extract.....	26
4.4. Synthesis of CuO and Co-doped CuO NMs	27
4.5. Characterization of CuO and Co-doped CuO NMs.....	27
4.5.1. Electrochemical analysis of CuO NMs.....	27

4.5.2. UV-Vis spectroscopy analysis of CuO NPs and Co-doped CuO NMs.....	28
4.5.3. FTIR analysis of CuO and Co-doped CuO NMs.....	30
4.5.4. XRD analysis of CuO and cobalt doped CuO NMs	32
4.5.5. Scanning electron microscopy (SEM) analysis of CuO and Co-doped CuO NMs..	34
4.6. Antimicrobial activity.....	36
4.6.1. Antibacterial activity.....	36
4.6.2. Antifungal activity.....	38
5. CONCLUSION AND RECOMMENDATION	39
5.1. Conclusion.....	39
5.2. Recommendation.....	40
6. REFERANCE.....	41
7. APPENDIX.....	51

LIST OF FIGURES	page
Figure 1. Application of green synthesis nanomaterials.....	7
Figure 2. Kalanchoe petitiiana.....	8
Figure 3. Application of k.petitiiana.....	8
Figure 4. Approaches for the synthesis of nanoparticles.....	12
Figure 5. Green synthesis of copper/copper oxide synthesis flow chart.....	13
Figure 6. Sample collection and preparation of plant extract.....	18
Figure 7. Phytochemical testing of plant extract.....	24
Figure 8. pH effects of CuO NMs.....	26
Figure 9. Cyclic voltammetry analysis.....	28
Figure 10 UV-Vis spectra of CuO NMs and energy band gap.....	29
Figure 11 UV-Vis spectra of 0.5% Co doped CuO NMs and energy band gap	29
Figure 12 UV-Vis spectra of 1% Co doped CuO NPS and energy band gap.....	29
Figure 13 UV-Vis spectra of 1.5% Co doped CuO NMs and energy band gap.....	30
Figure 14. FTIR analysis of plant extract and CuO NMs	31
Figure 15. FTIR analysis of CuO and Co-doped CuO NMs.....	32
Figure 16. XRD analysis of CuO NMs.....	33
Figure 17. XRD CuO and Co-doped CuO NMs analysis	34
Figure 18. SEM analysis of a and b respectively CuO and Co-doped CuO NMs.....	35
Figure 19. Zone of antibacterial activity.....	37
Figure 20. Zone of inhibition antifungal activity.....	38

LIST OF TABLE	page
Table 1 Phytochemical analysis.....	24
Table 2. XRD diffraction analysis of CuO and Co-doped CuO NMs.....	33
Table 3. Antibacterial test results.....	36
Table 4 . Antifungal test results.....	38

LIST OF ABBREVIATIONS

D	Average crystallite size
θ	Bragg's angle
CuO	Copper oxide
DIW	De-ionized water
DMSO	Dimethylsulfoxide
DW	Distilled water
E.coli	Escherichia coli
FTIR	Fourier Transform Infrared
β	Full width at half maxima of XRD spectral peak (in radians)
FWHM	Full Width at Half Maxima
IR	Infra-Red
Nps	Nanoparticles
SEM	Scanning electron microscopy
SERS	Surface-enhance Raman scattering
TEM	Transmission electron microscopy
UV-Vis	Ultra Violet Visible
XRD	X-ray Diffraction
λ	wavelength

ABSTRACT

Copper oxide nanoparticles have attracted huge attention due to their catalytic, electric, optical, photonic, and antimicrobial activity. The use of plant leaf extracts in the biosynthesis of nanostructured materials is an eco-friendly, non-toxic, and cost-effective approach.

In this study, green synthesis, characterization, and evaluation of the antimicrobial activity of copper oxide and Co-doped CuO NMs were studied by using Kalanchoe petitiiana leaf extracts. The CuO and Co-doped CuO NMs were successfully synthesized via a fast, convenient, cost-effective, and environmentally friendly method by biologically reducing 0.1M Cu(NO₃)₂·3H₂O and the dopant of Co(NO₃)₂·6H₂O solution with extract of kalanchoe petitiiana under optimum condition. The formation of Copper oxide nanoparticles was primarily noticed by observing color changes. The biosynthesized CuO and Co-doped CuONMs would be characterized by using UV-Vis analysis, Fourier Transform Infrared Analysis (FTIR), X-ray diffraction analysis (XRD), and scanning electron microscopy (SEM) and cyclic voltammetry (CV). From the UV-Vis absorption spectrum, the peaks of CuO NPs and Co-doped CuO Nps were detected at 230 and 227,231 and 228 nm respectively, and with E_g of 4.87, 4.85, 4.8, and 4.82 eV respectively. FT-IR revealed the presence of carbonyl and hydroxyl groups in the synthesized nanoparticles. The XRD data showed the crystalline structure of CuO NMs and Co-doped CuO NMs with crystallite sizes of 16.398, 16.393, 16.386, and 16.379nm respectively. SEM shows some CuO NMs has a spherical shape and Co-doped CuO NMs has a mixture of spherical and rod-like shape. CV shows oxidation-reduction reaction on oxidation at 0.3 v and reduction at -0.25 v. Evaluation of its antimicrobial activity against Gram-negative bacteria E.coli and S.typhi and Gram-positive bacteria S.aureus and B.Cereus and also antifungal activity against C.albicans. They were found to have a significant effect in controlling the growth of the human pathogens with a maximum inhibition zone of 25 mm and 24mm, 20 mm, and 19mm in S.typhi, S.aureus, B.Cereus and E. coli respectively and for C.albicans 20 mm indicates for CuONMs and Co-doped CuONMs also a zone of inhibition was increased after 24 h incubation time at 37°C.

Keywords: copper oxide nanoparticles, kalanchoe petitiiana, characterizations, antimicrobial activity.

1. INTRODUCTION

1.1. Background of the studies

Nanotechnology is the active area of research that deals with the size of materials that lie in the range of 1-100 nm. The particles with this range can be synthesized by various techniques. Synthesized particles may have a variety of shapes like nanospheres, nanorods, nanoribbons, nanobelts, and nanoplatelets [1]. In recent years, the Biosynthesis of nanoparticles is an important approach in nanotechnology. Nanotechnology has appealed to many researchers from several fields like biotechnology, physics, chemistry, material science, engineering, and medicine [2].

Nanomaterials are synthesized in different methods (physical, chemical, and biological), where biological methods are a good way to synthesize nanoparticles, and nanomaterials are used in multiple applications [3-9]. Biologically synthesized metal nanoparticles are stable and biosafety and also eco-friendly [10, 11]. Green chemistry is the design, development, and implementation of chemical products and processes to reduce or eliminate the use and generation of substances hazardous to human health and the environment. It was noted that strategies addressed environmental issues and related subjects, which in this case we have been pointed to the use of biodegradable polymers, environmentally benign solvents, and non-toxic chemicals [12].

In recent years, nanotechnology has illustrated the appropriate antibacterial capacities of metal nanoparticles/metal oxide nanoparticles compared to their bulk materials and common antibiotics. The copper oxide nanoparticle was acquired much importance because of less cost of synthesis has excellent chemical and physical properties very reactive because of its high surface area to volume ratio and easily interacts with other particles. These abilities can result from unique properties such as higher aspect ratio and surface area to volume ratio of these nanomaterials (NMs) compared with bulk materials [13].

Nanoparticles (NPs) are progressively utilized to target bacteria and fungi as a contrasting option to antibiotics. Bacterial infections are the endless cause of chronic infections and mortality Antibiotics played a very effective role in the treatment strategy for different infections, which are caused by bacteria due to their cost-effectiveness and intense results. Several investigations have given direct confirmation that the broad spectrum utilization of antibiotics creates the generation of the strains of multidrug-resistant bacteria and fungi. The super bacteria and fungi are types of microbial strains that show resistance against all the antibiotics, which have been developed recently because of the abuse of antibiotics. Copper oxide nanoparticles are toxic for many microorganisms such as *Escherichia coli*, and *Staphylococcus aureus* and non-toxic for animal cells. The main groups of antibiotics are presently being used actively in three different modes of the synthesis of the cell wall, translational,

and the deoxyribonucleic acid (DNA) replication mechanisms. Bacteria are resistant to all these modes of action [14].

In recent years, using metal oxide nanoparticles as adsorbents has been receiving special attention because of their great specific surface area and porous nature for the removal of synthetic dyestuffs from aqueous solutions by adsorption. Copper oxide (CuO) is a significant industrial material for wide variety of applications such as heterogeneous catalysis, electrode material, gas sensors, magnetic storage media, semiconductors, solar cells, solar energy transformation, and reactive oxidizers in nanothermite composites [15]. Green synthesis has numerous advantages, compared to other methods, including cost-effectiveness, simplicity, use of lower temperatures, use of non-toxic materials, as well as compatibility with applied medical and food applications [16].

Copper oxide nanoparticles exhibit high potentiality in the metal oxide NPs owing to their antimicrobial, catalytic, optical, and low-cost properties. Copper oxide NPs have a band gap ranging from 1.35-3.5 eV. Due to their suitable band gap, easy availability, low toxicity, and surface synthesis among different semiconductor photocatalysts [17]. In general, metal-doping induces drastic changes in optical, electrical, and magnetic properties of CuO by altering its electronic structure. Many authors have reported the changes associated with doping of transition metal ions into CuO lattice, including Fe, Mn, Fe, and Ni Co-doped Ti, Cd, and Zn. Although, there have been a large number of reports on transition metal doped CuO systems, literature on Co-doped CuO is scarce [18].

Biosynthesis of metal oxide nanoparticles by plants is currently under development. The synthesis of metal oxide nanoparticles using inactivated plant tissue, plant extracts, exudates, and other parts of living plants is a modern alternative for their production [19]. In the biosynthesis of metallic nanoparticles using plant extract, three important parameters are metal salt, a reducing agent, and a stabilizing or capping agent for controlling the size of nanoparticles and preventing their aggregation [20].

Many biomolecules in plants such as proteins/enzymes, amino acids, carbohydrates, alkaloids, terpenoids, tannins, saponins, and phenolic compounds, reducing sugar, and vitamins and could be involved in bioreduction, formation, and stabilization of metal nanoparticles [21]. The reduction potential of ions and reducing the capacity of plants which depend on the presence of polyphenols, enzymes, and other chelating agents present in plants have critical effects on the amounts of nanoparticle production.

Among all nanoparticles preparation with plant extracts has attracted massive attention due to the accessibility of a biological entity. Based on the previous literature reports, CuO nanoparticles

were synthesized from various plant extracts such as Aloe Vera leaves, Carica papaya leaves, tea leaves, and coffee powder, Albizia lebbek leaves, Abutilon indicum Leaf Extract was reported for the CuO nanoparticless in recent years [22]. To the best knowledge, copper oxide nanoparticles synthesis with *kalanchoe petitiiana* leaf extract is not reported. In this study, the synthesis of copper oxide nanoparticles and cobalt doper oxide from leave extracts of plant *kalanchoe petitiiana* was selected due to its potential medicinal value.

1.2.Statement of the problem

During the last decade, a rapid increment in the development of new antibacterial materials has been observed as a consequence of the spread of antibiotic-resistant infections, which has become a major issue in health care. The emerging infectious diseases and the development of drug-resistant bacteria at an alarming rate is a matter of serious concern and an increasing public health problem. New strategies for controlling bacterial activity are urgently needed and nanomaterials can be a very promising approach. A possible alternative is the synthesis of new inorganic compounds with antimicrobial properties. Copper oxide nanoparticle has the advantage of durability as well as chemical and physical stability over common organics and antibiotics compounds.

Unfortunately, the use of toxic organic solvents and strong reducing agents results in producing hazardous wastes which pose a great risk to the environment. Furthermore, conventional synthesis of metallic oxide nanoparticles is often time-consuming unlike green synthesis methods and biological synthesis is formed for a short period, with low costs, and safety. Many research works had been concerned with the green synthesis of nanoparticles for antibacterial applications which is the recent research focus.

Many researchers reported that new multi-drug resistance (MDR) strains of bacteria have yet developed and become a serious problem in public health. To fill this gap, there should be effective, economically feasible, and broadly applicable new drugs. Green synthesis of nanoparticles using plant leaf extracts are among the main area for research of new antimicrobial agents. In this study, *kalanchoe petitiiana* leaf extract is used to synthesize CuO NMs and Co-doped CuO NMs, and its antimicrobial activity was evaluated. However, to the best of our knowledge, there is no study conducted on the biogenic synthesis of CuO and Co-doped CuO NMs by using *kalanchoe petitiiana* leaf extract so this could be taken as the first study and a good opportunity to test its antimicrobial activity.

Thus the present study may intend to evaluate the antimicrobial application of CuO and Co-dope CuO NMs supported by *Kalanchoe petitiiana* extract that may answer the following questions.

1. Is *Kalanchoe petitiiana* leave extract used as a reducing and capping agent for the synthesis of CuO NMs and Co-doped CuO NMs?

2. Is the synthesized CuO and Co-doped CuONMs efficient for antimicrobial activity?

1.3. Objectives

1.3.1. General objective

The general objective of this study is a green synthesis of CuO and Co-doped CuO NMs using an aqueous extract of *kalanchoe pettitiana* leaves and to evaluate its antimicrobial activity.

1.3.2. Specific objectives

The specific objectives of this study were:

- To prepare *Kalanchoe pettitiana* leaves extract.
- To conduct a phytochemical screening test
- To synthesize CuO and Co-doped CuO NMs using *kalanchoe pettitiana* leave extract as reducing and capping agents.
- To characterize the synthesized CuO and Co-doped CuO NMs using XRD, SEM, CV, FT-IR, and UV- Visible techniques.
- To evaluate the antimicrobial activity of the synthesized copper oxide and Co-doped CuO NMs against *Salmonella typhi*, *Bacillus cereus*, *Staphylococcus aureus*, and *Escherichia coli* and fungus such as *C.albicans*

1.4. Significance of the study

The green synthesis of nanoparticles using plant extract is an active area of current research, attracting the interest of many researchers because of their wide applications. The major advantage of green synthesis of nanoparticles is their important role in protecting the environment and also the synthesized particles are stable.

Nowadays due to the expansion of water pollution and multidrug-resistant bacteria, the synthesis of nanoparticles is highly important. The most preferred method for the synthesis of nanoparticles is the use of biological entities like bacteria, yeast, fungi, and plants. However, plant extract-mediated synthesis is potentially advantageous over microorganisms due to the ease of scale-up, safe, simple, and environment friendly. Plant extracts are a broad variety of metabolites that can be used in the reduction of metal ions, capping, and stabilizing agents for the nanoparticles. Therefore, the finding of this study was used:

- ❖ To provide an economically feasible option to produce extract crude (*indahula*) locally, which was play a major role to substitute the imported synthetic medicine.
- ❖ To enhance the knowledge about CuO NMs and Co-doped CuO NMs regarding their antimicrobial activities.

- ❖ To set the foundation for further investigation of applications of CuO NMs and Co-doped CuO NMs.
- ❖ Providing further awareness for researchers about the antimicrobial action of CuO and Co-doped CuO NMs.

2. LITERATURE REVIEW

2.1. Overview of nanoparticles, nanotechnology, and nanoscience

A nanoparticle is a core particle that performs as a whole unit in terms of transport and property [23]. As the name indicates nano means a billionth or 10^{-9} unit and with its small size it occupies a position in various fields of nanoscience and nanotechnology. The term "nanoparticles" is used to describe a particle with a size in the range of 1nm-100nm, at least in one of the three possible dimensions. In this size range, the physical, chemical, and biological properties of the nanoparticles changes in fundamental ways from the properties of both individual atoms/molecules and of the corresponding bulk materials [24]. Nanoparticles are characterized by an extremely large surface area to volume ratio, and their properties are determined mainly by the behavior of their surface [25]. The applications of nanoparticles are well known in the fields of cosmetics and pharmaceutical products, coatings, electronics, polishing, semiconductors, and catalysis. The design and preparation of novel nanomaterials with tunable physical and chemical properties remain a growing area.

Nanotechnology is the application of science and technology to control matter at the molecular level, which is also referred to as the ability for designing, producing, characterizing, and applying to structures, devices, and systems by controlling shape and size at the nanometer scale [26]. Nanotechnology emerges from the physical, chemical, biological, and engineering sciences where novel techniques are being developed to probe and manipulate single atoms and molecules. Nanoscience is a new interdisciplinary subject that depends on the fundamental properties of nano-size objects [27].

NMs are defined as materials with at least one external dimension in the size range from approximately 1-100 nanometers. A focused integration of bio and nano techniques for the biological synthesis of NMs, known as bionanotechnology, has emerged from nanotechnology [28]. Biological synthesis combines biological principles (i.e., reduction/oxidation) by microbial enzymes or plant phytochemicals with physical and chemical approaches to produce nano-sized particles. Nanomaterials have broad applications in a variety of fields because of their unusual and size-dependent optical, magnetic, electronic, and chemical properties [29]. Nanomaterials can show atom-like behaviors which result from higher surface energy due to their large surface area, while a bulk material has constant physical properties regardless of its size, at the nanoscale, this is often not the case [30].

2.2. Need for green synthesis

Biosynthesis of nanoparticles is a kind of bottom-up approach where the main reaction occurring is reduction/oxidation. The need for the biosynthesis of nanoparticles rose as the physical and chemical processes were costly. Often, the chemical synthesis method leads to the presence of some toxic chemical absorbed on the surface that may harm medical applications [31]. This is not an issue when it comes to biosynthesized nanoparticles via the green synthesis route [32]. So, in the search for cheaper pathways for nanoparticle synthesis, scientists used microbial enzymes and plant extracts (phytochemicals), and their antioxidant or reducing properties are usually responsible for the reduction of metal compounds into their respective nanoparticles. Green synthesis provides advancement over chemical and physical methods as it is cost-effective, environment friendly, and easily scaled up for large-scale synthesis, and in this method, there is no need to use high pressure, energy, temperature, and toxic chemicals.

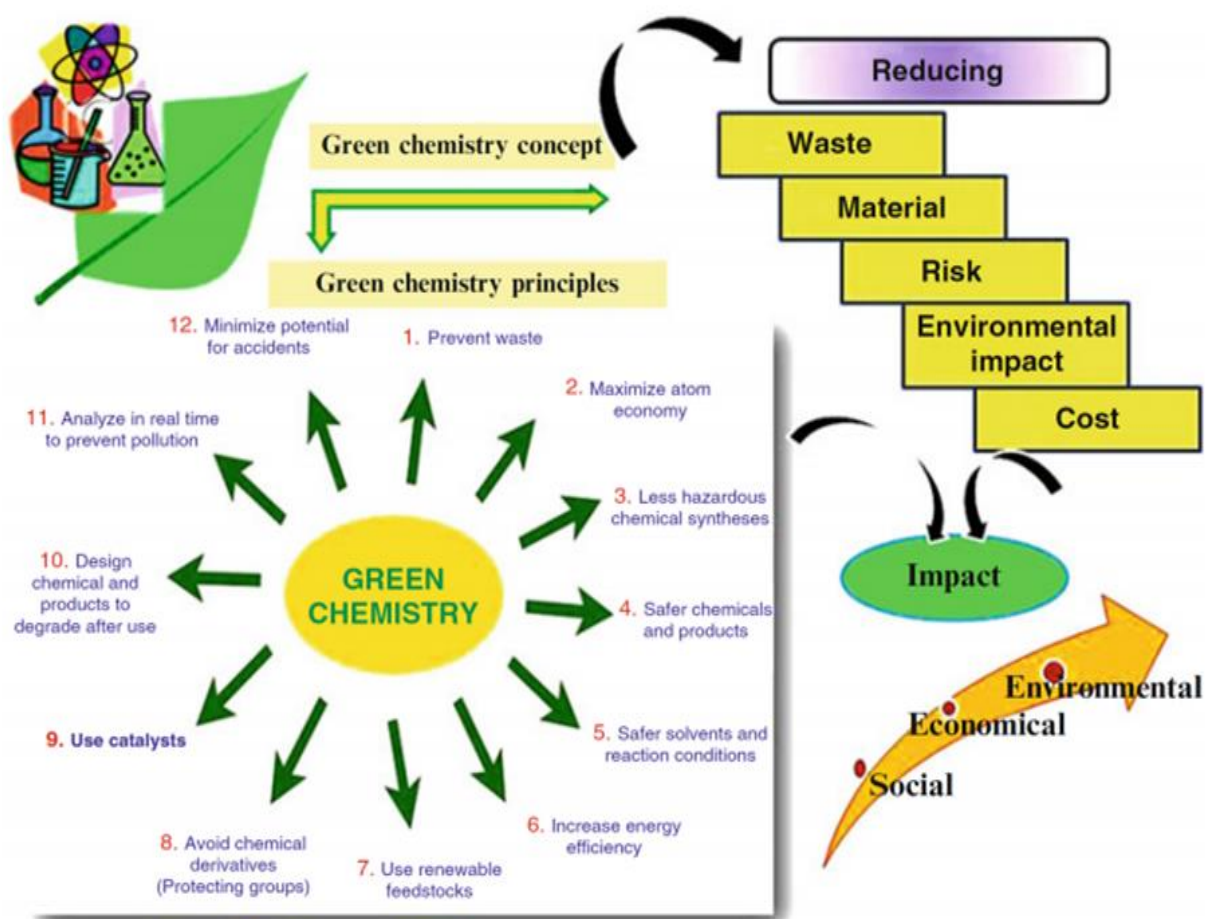


Figure 1. Application of green synthesis nanoparticles [33]

2.3. About *Kalanchoe petitiiana*

Kalanchoe petitiiana is a species of succulent plant that belongs to the family Crassulaceae [34]. It was native to Ethiopia and here it is commonly called indahula in Amharic [35]. For optimum growth, the plant prefers a sunny to partly-shady condition on fresh to moist soil, with a temperature above 1 °C.



Figure 2. *Kalanchoe petitiiana*

2.4. Pharmacological medicinal use of *Kalanchoe petitiiana*

Different parts of the plant are used for treating many disease conditions in Ethiopian traditional medicine. These conditions include epilepsy, trachoma, allergy, intestinal parasites, gonorrhoea, malignant wounds, breast tumor, and skin cancer. The leaves of the plant are used for treating both forms of cancer such as breast cancer and skin cancer. Confirming the anticancer effect reported, gallic acid with potent antitumor activity is isolated from the leaves of *K. petitiiana* [35].

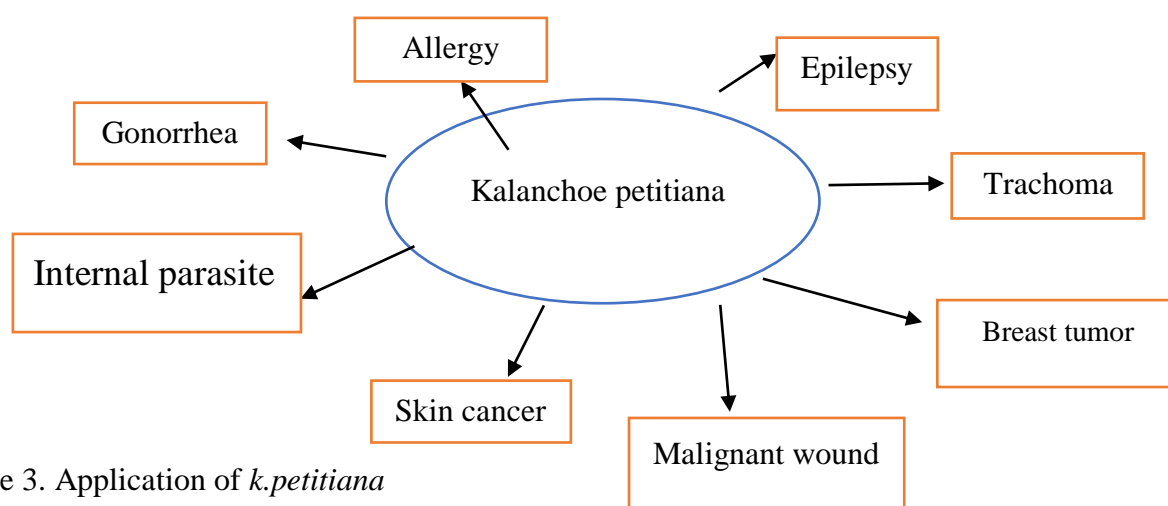


Figure 3. Application of *k.petitiiana*

2.5. CuO and Co-doped Copper oxide nanomaterials

The metal oxide (MO) nanomaterials have received specific research attention from researchers owing to their different properties such as their catalytic, magnetic, electronic, optical, biological, and medicinal properties as compared to their bulk counterparts. Among all the transition metal

oxides, CuO nanoparticles have received more attention because of their outstanding physical and chemical properties. Copper oxide is composed of two main elements copper and oxygen that belong to the d and p blocks, respectively. Copper oxide (CuO) nanoparticles show high catalytic activity and selectivity as compared to their bulk counterparts owing to their large surface to volume ratio. CuO nanostructures are well-known antibacterial materials and find applications in various fields such as superconductors, photocatalytic degradation, gas sensors, and biosensors[36].

Exploration of CuO nanoparticles is few compared to other transition metal oxides like ZnO, SnO₂, TiO₂, and Fe₂O₃ making it an interesting material to study. Altering the characteristics of the material by doping the semiconductor nanoparticles with metal ions is one of the most significant methods. The influence on physical, chemical, and electronic properties of the semiconductors by the engineering of the band gap is possible by making use of the accurate dopants [37].

Many transition metals have been used for doping, Co-doping of pure CuO nanoparticles to change their physical and chemical properties. Doping with metallic atoms on pure CuO nanoparticles can be used to improve the physical properties of pure CuO nanoparticles and the ions doping on the pure CuO nanoparticles can improve the photocatalytic activity of CuO nanoparticles [38].

In general, when metal oxide NPs are doped with transition metals, the particle size gets reduced and which in turn increases the rate of the catalytic reduction reaction. Besides, whenever transition metals are doped in metal oxides, the lattice defects are observed which significantly affects the charge transfer processes to ease catalytic reactions [36]. Cobalt (Co²⁺) is taken as a dopant because the ionic radii of Cobalt (0.72 Å) are almost similar to Cu²⁺ (0.71 Å). CuO: Co NPs show high chemical reactivity to produce more active sites for reduction reactions. so far the effect of doping or Co-doping on transition metals such as Fe, ZrO₂, Fe/Co, Ni, Fe/Ni, Mn, Mn/Co, and La/Ni [39].

2.6. Biomedical applications of copper oxide nanomaterials

CuO NMs have diverse scientific applications. They are very effective against different pathogenic microbes. Among all other nanoparticles, copper oxide (CuO) nanoparticles get much attention because of their multifarious applications. It possesses various properties and has diverse applications. General applications of copper oxide include biomedical(antimicrobial, anti-fouling, antifungal, antibiotics, antioxidants, drug delivery, and anticancer), textile industries, thermo sensing and conducting materials, gas sensors, catalytic, synthesis of inorganic-organic nanosize

composites, magneto resistant materials, high-temperature superconductor, environmental remediation, etc [40].

2.6.1. Antibacterial activity

In the past few years, nano-based therapies have been used to diagnose and treat diseases and formulate novel drugs. The antibacterial activities of nanoparticles have been tested against different pathogenic bacterial strains and showed substantial outcomes. Literature reports reveal that CuONMs are highly toxic to most human pathogens. Bio fabricated copper oxide nanoparticles have attracted great interest as antibacterial agents due to their unique morphologies, size, and bio-compatible nature to treat a wide range of pathogenic human bacteria. The green synthesized copper oxide nanoparticles also possess vigorous antibacterial activities against both Gram-positive and Gram-negative bacterial strains. The green synthesis of copper oxide nanoparticles using leaf extract of *k.petitiana* and evaluated their antimicrobial activities. The copper oxide nanoparticles generate reactive oxygen species (ROS), which interact with the cell membrane of bacteria to enter the cell which results in the inhibition of bacterial cell growth due to the disturbance in the cell membrane that might lead to death. The copper oxide nanoparticles destroy the cell membrane of bacteria through ROS production or by direct cell damage as the metal oxide nanoparticles (CuO) produce superoxide and hydroxyl radicals. Copper oxide nanoparticles also cause DNA and protein damage, prevents biofilm production, damage proton efflux pumps, and oxidize bacterial cells' cellular substances[41].

2.6.2. Antifungal activity

In the current medical history, the fungal disease has become a significant health problem, especially among patients having a weak immune system such as AIDS or cancer patients undergoing chemical treatment. The antifungal activity of copper oxide nanoparticles has been investigated for medical applications that these nanoparticles may combat fungal infections. However, the antifungal activities of copper oxide nanoparticles have been less studied as compared to antibacterial activity[42].

2.7. Techniques of synthesis of CuO and Co-doped CuO nanomaterials

Nanoparticles can be formed by two approaches: top-down (comminution and dispersion) or bottom-up (nucleation and growth) and both of them have their limitation and advantages in producing nanomaterials.

2.7.1. Top-down approach

In general, a process of producing desired patterns on micro or nano-scale through lithographic methods or bulk that breaks down to smaller particles is called a top-down approach. Usually, physical methods such as arc discharge, pulsed laser ablation, and hydrometallurgy are assorted in this type of approach. The advantages of using this type of approach are easy to conduct and it could produce stable nanoparticles without the involvement of a stabilizer or capping agent. However, this kind of approach has its limitation where it needs a high amount of energy and also high costs of equipment. Due to the high energy, the physicochemical properties of nanoparticles and their surface might be defected [42].

2.7.2. Bottom-up approaches

The bottom-up approach could be defined when the nanoparticles are obtained from atoms, molecules, and small particles or monomers (precursors). These basic building blocks of precursors are self-assembled precisely and fit together to produce nanoparticles. As this kind of approach could give the ability to control terms of size, shape, and morphology of nanoparticles, hence, it become more favorable for synthesizing nanoparticles nowadays. Typically, the bottom-up approach comprises the chemical and biosynthesis procedure for synthesizing nanoparticles such as chemical reduction, gamma irradiation, microwave irradiation, and sonochemical and plant-based synthesis method. Several of these methods have their strength and weaknesses. As for the disadvantages, the limitation of the machine is one of the problems for the physical method. While in chemical routes like chemical vapor deposition and chemical reduction, the major drawback is the involvement of toxic chemicals such as hydrazine and sodium boron hydride that could harm the environment and are unsuitable for applications. Preparation of nanoparticles using a chemical route may cause an adverse effect in the medical application as the presence of toxic chemicals may absorb on the surface of the nanoparticles. Therefore, green synthesis has been popular among the research studies currently as it consists a lot of benefits, especially it could eliminate the use of environmental risk substances which is good for biomedical applications specifically and also the advantages are low cost, simple, less time-consuming method and non-toxic [42].

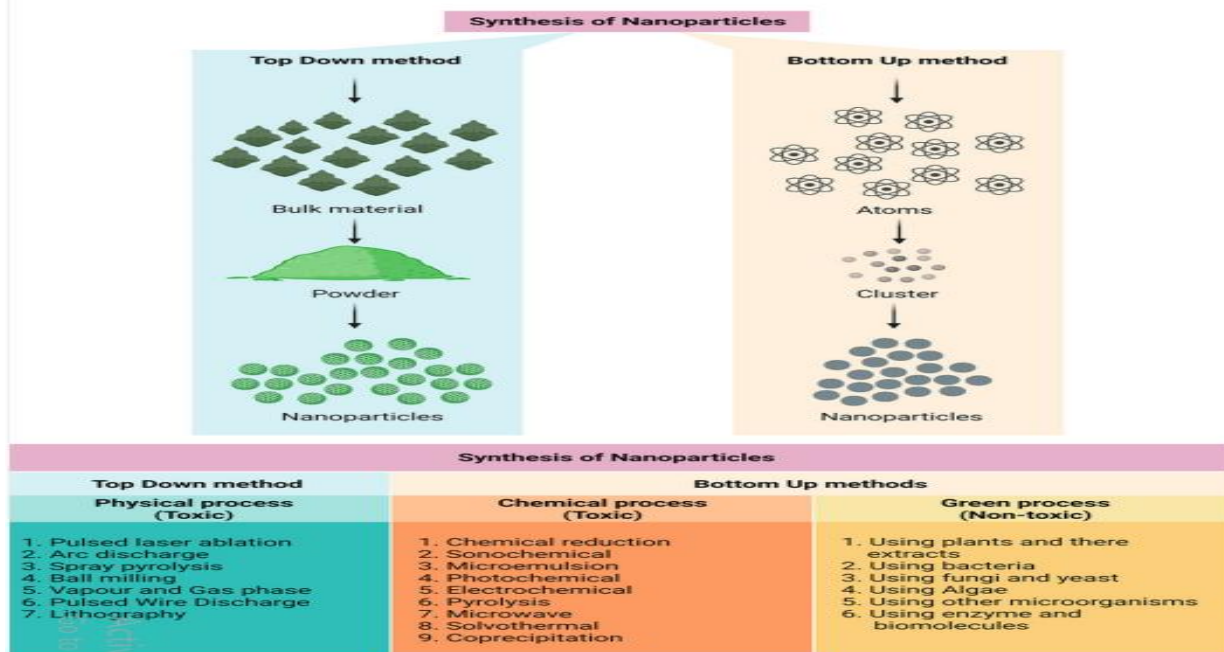


Figure 4. Approaches for the synthesis of nanoparticles[43]

2.8. Biosynthesis of CuO and Co-doped CuO nanomaterials

The presence of different organic and inorganic pollutants in water due to industrial, agricultural, and domestic activities has led to a global need for the development of new, improved, and advanced technologies that can effectively improve water quality [44]. In nanotechnology, the development of the controlled synthesis of nanoparticles with well-defined shape, size, and composition is a big challenge. Metallic nanoparticles exhibit unique properties when compared with conventional metallic materials. This could be utilized in many new interesting applications such as biomedical sciences and electronics industries [45]. Biosynthesis of nanoparticles was developed to overcome the problems of physical and chemical synthesis like cost and hazardous chemicals.

Although chemical & physical methods are very successful to produce well-defined nanoparticles, they have certain drawbacks such as increased cost of production, the release of hazardous by-products, long time for synthesis, and difficulty in purification [46]. Global warming & climate change has induced a worldwide awareness to reduce the toxic & hazardous waste materials, thus, the green synthesis route has raised actively the progress in the fields of science & industry [47]. The use of biological organisms such as a microorganism, plant extracts, and biomass could be the best alternative method to the physical and chemical method for the synthesis of nanoparticles because the biological or green synthesis way is very spontaneous, economic, environmentally friendly, and non-toxic. Therefore, biological sources such as bacteria, fungi, yeasts, algae, and

plants can materials catalyze specific reactions as a part of a modern & realistic biosynthetic strategy.

The current perspective on the biological system has created commercial importance due to its enzymatic reactions, photochemical characteristics, and herbal nature. The biological system has created a specific and revolutionary change for the synthesis of nanoparticles due to their mode of the mechanism through which the bioreduction of the metallic salts occurs is still a mystery. Numerous researches have been done on the synthesis of nanoparticles from the biological system for their application in the field of biomedical, pharmaceutical, cosmetic and environmental use. Bio fabricated nanoparticles can be used for bioremediation purposes because nanoparticles can diffuse or penetrate through the contaminants and cause a redox reaction to clean the surface materials. Nature has some processed devices for the synthesis of nano and micro-sized materials which contribute to the development of the relatively new and unexplored areas of research based on the biosynthesis of nanomaterials

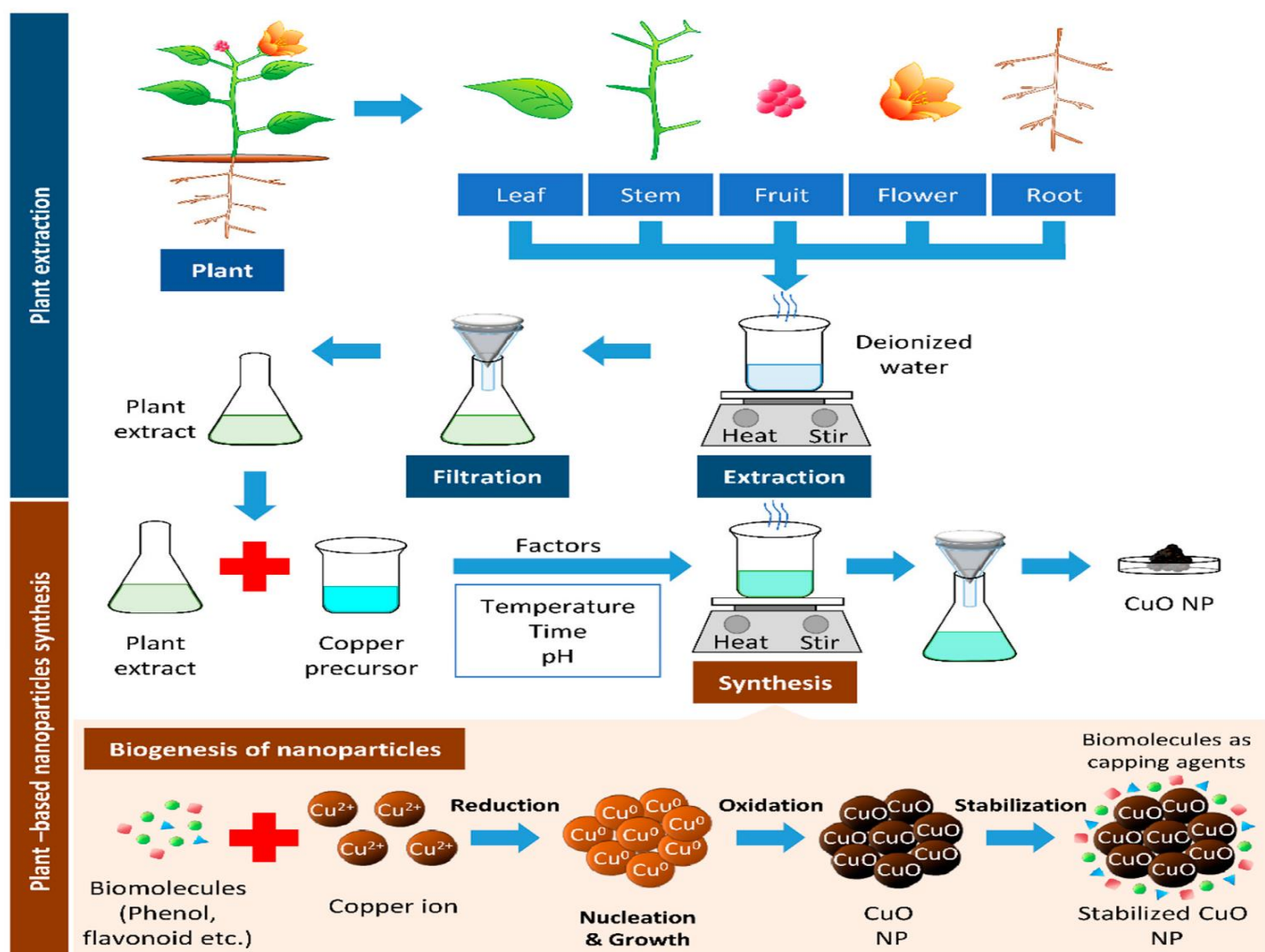


Figure 5. Green synthesis of copper/copper oxide synthesis flow chart[48]

2.9. Factors affecting biosynthesis of nanoparticles

Several factors such as pH, temperature, the concentration of plant extract, the concentration of the metal solution, incubation/reaction time, etc, affect the synthesis, size, and shape of nanoparticles. Free surface electrons of uncapped nanoparticles are highly reactive which makes and may promote aggregation. The stability, functionality, and applications are significant for the incorporation of nanoparticles with biological molecules.

2.9.1. Concentration of Plant Extracts

The synthesis of CuO nanoparticles using plants extract depends majorly on the types of biomolecules found in plant extracts and the volume used [49]. The biomolecules in plant extracts can act as natural capping and reducing agents during the green synthesis of NPs. These metabolite compositions vary depending on the types and parts of the plant and the extraction procedure [50]. Hence, the volume of plant extracts and the number of biomolecules present in the plant extract used can affect the synthesis rate due to the availability of these molecules for the rapid bioreduction of metal salts and the stabilization of NPs [51]. It was demonstrated that increased concentrations of plant extract speed up the rate of reduction of copper ions in the solution, which directly increases the formation rate of Cu and CuO NPs [52]. This is attributed to the phytochemicals present in the plant extract, which are responsible for the bioreduction and stabilization of the NPs [52]. In addition to speeding up the reaction, an increase in the concentration of plant extract also decreases the size and alters the shape of the CuO NPs formed. A recent study demonstrated that synthesizing CuO NPs using a different volume of sugarcane juice, ranging from 2–10 mL, produced CuO NPs that were 29.89–22.80 nm in size [52]. Notably, the CuO NPs synthesized were spherical when using a higher concentration of sugarcane juices. In contrast, various shapes were observed from the CuO NPs synthesized with lower concentrations of sugarcane juice, ranging from spherical, square, cube, and plate shapes to rectangular shapes, along with some irregular shapes [53]. This is supported by previous studies demonstrating that increasing the concentration of plant extract when synthesizing NPs alters NP morphology, from irregular to spherical, and the size of the NPs [52].

2.9.2. Precursor Used

The precursor is a salt and alkali metal solution. Numerous soluble copper salts were used in the green synthesis of Cu and CuO NPs, such as copper chloride (CuCl_2), copper sulfate (CuSO_4), and copper acetate ($\text{Cu}(\text{OAc})_2$), and copper nitrate ($\text{Cu}(\text{NO}_3)_2$). Copper salts are the primary source for releasing Cu^{2+} ions in reaction mixtures; the bioreduction of these ions by the plant extracts forms the complete NP [52]. When changing the precursor has no significant impact on the crystal

structures of CuO NPs. It was also revealed that a low concentration of the precursor produced smaller-sized NPs, whereas a high concentration of the precursor produced larger NPs with faster agglomeration [54].

2.9.3. pH measurements

The pH of the reacting mixture in the biosynthesis of NPs is also one of the factors affecting the size of NPs. The optimum pH of the reaction medium ranges from 8 to 9, suggesting an alkaline condition is favorable for synthesizing NPs [55]. Biosynthesis of NPs occurring at the alkaline condition of $\text{pH} > 8$ produces smaller-sized NPs. The NPs synthesized in an acidic condition of $\text{pH} < 7$ were a relatively larger particle size. The synthesis of CuO NPs at alkaline produces loosely agglomerated NPs, with sharp CuO NPs with smaller particle sizes. In an acidic or neutral condition, more agglomerated CuO NPs, with larger particle sizes [56].

2.10. Characterization technique

Nanoparticles are characterized using UV-Vis absorption spectroscopy FTIR, XRD, SEM, TEM, CV, etc. technique

2.10.1. UV-Visible absorption techniques

The formations of metal nanoparticles are monitored by UV-Visible spectroscopy as colloidal dispersions of metal show absorption bands in the UV-Visible range due to the excitation of plasma resonances or interband transitions, characteristic properties of the metallic nature of the particles. UV-visible absorption spectroscopy:

Absorbance spectroscopy is used to determine the optical properties of a solution. A Light is sent through the sample solution and the amount of absorbed light is measured. When the wavelength is varied and the absorbance is measured at each wavelength. The absorbance can be used to measure the concentration of a solution by using the Beer-Lamberts Law. The optical measurement of UV-visible spectrophotometer has a different absorbance peak like 410 nm when treated with the *Nerium Obander* plant extract after the addition of aqueous 1mM Silver nitrate solution [54]. In the case of *Azadirachta indica* get synthesized with Iron nanoparticles by the indication of suitable surface Plasmon resonance with high band intensities and peaks was found through UV-visible spectroscopy at the range of 216-265 nm [55].

2.10.2 X-ray diffraction (XRD) techniques

X-ray diffraction is a conventional technique for the determination of crystallographic structure and morphology. There is an increase or decrease in intensity with the amount of constituent. This technique is used to establish the metallic nature of particles gives information on translational

symmetry size and shape of the unit cell from peak positions and information on electron density inside the unit cell, namely where the atoms are located from peak intensities.

2.10.3. Fourier transform infrared (FTIR) spectroscopy

Measures infrared intensity vs. wavelength of light, it is used to determine the nature of associated functional groups and structural features of biological extracts with nanoparticles. The calculated spectra reflect the well-known dependence of nanoparticle optical properties. The green synthesized silver nanoparticle by employing various leaf extracts was analyzed using Fourier Transform Infrared [FTIR] Spectroscopy and showed characteristic peaks. [56].

2.10.4. Electrochemical Studies

The cyclic voltammetry was used to identify the oxidation and reduction reactions (redox reactions) by using a potentiostat with a three-electrode system. CV was also used to identify catalytic reactions. Drop Sense with inbuilt Drop view 200 software (Metrohm South Africa (Pty) Ltd., Johannesburg, South Africa) was fitted with screen printed carbon electrode (SPC) having an inner carbon working electrode (diameter of 4 mm), a silver pseudo-reference (Ag/AgCl) electrode (RE) and carbon counter electrode (CE). SPC was modified with CuO to obtain the modified working electrode used for the electrochemical studies [57].

2.11. Applications of nanoparticles to human health and environments

The main application involved in the use of nanoparticles for biomedical applications, such as drug and gene delivery, cancer treatment and diagnostic tools, food, etc. has been extensively studied throughout the past decade and also nanoparticles created huge interest due to their very small size and large surface-to-volume ratio, and they display novel uniqueness contrast to the large particles of bulk material [58].

3. MATERIAL AND METHODS

3.1. Study area

The study was carried out at Jimma University's main campus, Chemistry Research Laboratory which is located 346 km away from Addis Ababa, Ethiopia.

3.1.1. Materials

Magnetic stirrer, mortar, and pestle, water bath, deionizer, Refrigerator, Petri dish, Inoculating needles, digital balance, conical flask, beaker, centrifugation tubes, volumetric flask, pipettes, Pyrex glass, Erlenmeyer flask, Whatman filter paper No-1, Watch, funnel, Test tubes, Droppers, Graduated cylinders, Glass rode, Cuvettes, Aluminium foil, spatula, micropipette, desiccators, hot plate, polyethylene bags were used for the present study.

3.1.2. Chemicals and reagents

Copper nitrate trihydrate $\text{Cu}(\text{NO}_3)_2 \cdot 3\text{H}_2\text{O}$ as a precursor, $\text{Co}(\text{NO}_3)_2 \cdot 6\text{H}_2\text{O}$ as a dopant, NaOH, Ferric chloride(anhydride)(FeCl_3), dilute hydrochloric acid (HCl), potassium iodide and iodide as a reagent, nutrient agar media for bacteria growth, DMSO, Gentamicin, and Clitromazol as a controller, de-ionized water(DI) and plant leave extracts as reducing and the stabilizing agent was used for the synthesis of CuO and Co-doped CuO NMss.

3.1.3. Instruments

UV-Visible spectroscopy (JENWAY6705 UV-Vis spectroscopy) Jimma university organic and inorganic laboratory, XRD-7000, Jimma university material science department, Fourier transforms infrared spectroscopy (FTIR) Shimadzu IR-470 Spectrometer (Shimadzu, Japan); pH meter (Jimma university organic and inorganic laboratory), SEM (transmission electron microscopy), CV (Cyclic voltammetry) were used for present study.

3.2. Sample collection and preparation of plant extract

25 g of *kalanchoe petitiiana* leaf was collected from the Mizan Aman, Mizan town local name is Ediget Keble, and SNNP region state Ethiopia in September 2021. The collected sample was washed thoroughly with distilled water to remove the dust particles if any adsorbed on the surface of the leaves and the washed samples were air-dried. The dried leaves were crushed with mortar and pestle. After crushing 3 gm of the ground leaves along with 100 mL of distilled water were heated on a hot plate at 70 °C for 30 min. After the formation of the plant extract, it was filtered using Whatman No.1 filter paper, and then the freshly prepared extract was used for the synthesis of CuO and Co-doped CuO NMs. The resulting sample leaf extract was kept at 4 °C [59].

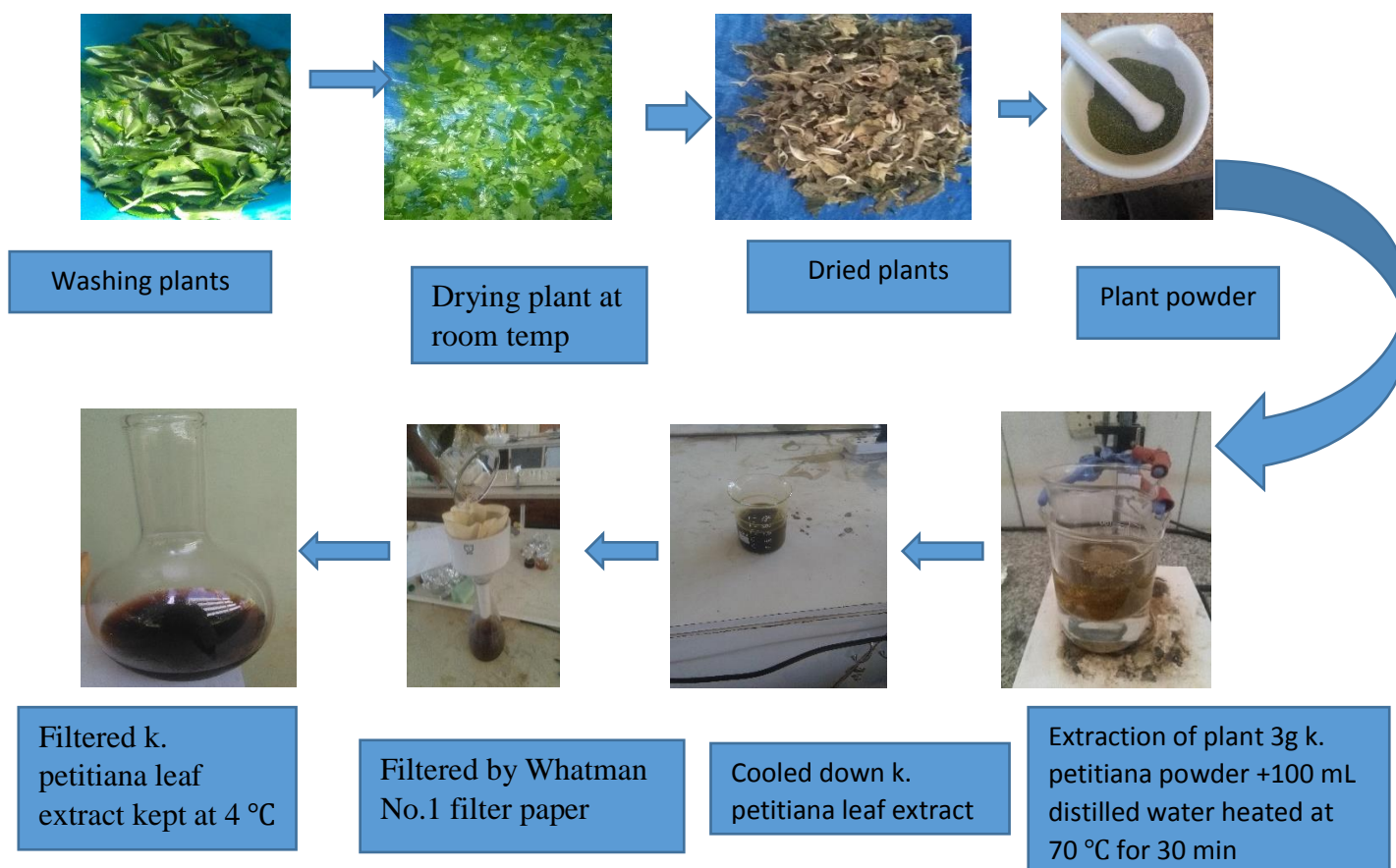


Figure 6. Sample collection and preparation of plant extract

3.3. Qualitative Phytochemical Screening

Phytochemical screening of freshly prepared *kalanchoe petitiana* leaf extract was carried out using simple chemical tests to identify the presence of active phytoconstituents i.e. polyphenols, alkaloids, flavonoids, saponins, tannins, etc. in the sample[60,61]

1. Test for flavonoids (alkaline reagent test)

Extracts were treated with a few drops of 20% sodium hydroxide solution. The formation of an intense yellow color, which turns colorless on the addition of dilute hydrochloric acid, indicates the presence of flavonoids.

2. Test for alkaloids (Wagner's test)

The plant extracts were treated with a few drops of Wagner's reagent (0.5 g of iodine and 1.5 g of potassium iodide were dissolved in 5 mL of distilled water and the solution was diluted to 20 mL using water). The formation of reddish brown precipitate indicated the presence of alkaloids.

3. Test for phenols

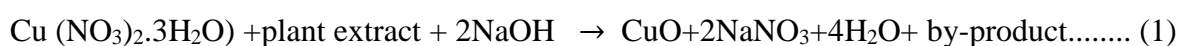
5 mL of leaf extract with a few drops of 5% neutral FeCl_3 solution was added and a dark green color was formed indicating the presence of Phenolic Compounds.

3.4. Optimization of copper oxide nanomaterials

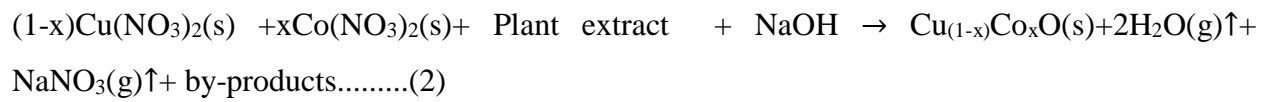
The concentration ratio of leaf extract and copper nitrate solution was optimized with the increase in the concentration of leaf extract (10, 20, 30 mL) in 40 mL of 0.1 M copper nitrate solutions (ratio 1:4, 1:2, 3:4). After 3 h of incubation, the absorbance of the resulting solution was measured UV-Visible spectrometer. The concentration ratio of leaf extract and copper nitrate was optimized with the increase in the concentration of copper nitrate solution (0.05, 0.1, and 0.15 M) in a constant volume of leaf extract (20 mL) and pH-9. The reaction mixture was incubated for 3 h and the absorbance of the resulting solution was measured UV-Visible spectrometer. The pH of the reaction was optimized by increasing the pH value was 5, 7, 9, and 11 and the remaining volume of plant extract and concentration of precursor was constant and it was adjusted using 2 M NaOH and diluted HCl acids. The effect of these parameters on the synthesis of CuO NPs was monitored by using a UV-Visible spectrometer [62, 63].

3.5. Biosynthesis of CuO and Co-doped copper oxide nanomaterials

Synthesis of CuO NPs capped with *kalanchoe petitiiana* leaf extract was conducted according to the reported literature with slight modifications. 0.1 M $\text{Cu}(\text{NO}_3)_2 \cdot 3\text{H}_2\text{O}$, 0.97 g of copper (II) nitrate trihydrate was dissolved in 40 mL of deionized water, and solution was added to freshly prepared 20 mL of the *kalanchoe petitiiana* leaf extract. To adjust pH-9, 5 g of sodium hydroxide (2 M NaOH) was separately dissolved in 60 mL of distilled water after that added drop by drop until pH was adjusted and stirred using a magnetic stirrer at 600 rpm for 3 h at 70 °C then the deep blue color of the copper nitrate solution was changed to light green on the addition of plant extract (Appendix 1). After 3 h, a green colored nanoparticle was formed which indicates the formation of CuO NPs.



The final solution was centrifuged well for 20 min at 3000 rpm, and the solution was multi-washed with double distilled water and ethanol it was poured into the Petri dish and kept in the oven at 80 °C for 1 h for further study. For 0.5% of cobalt doped copper oxide nanoparticles, each 0.1 M $\text{Cu}(\text{NO}_3)_2 \cdot 3\text{H}_2\text{O}$, 0.97 g of copper (II) nitrate trihydrate was dissolved in 40 mL of deionized water and 0.5 g of $\text{Co}(\text{NO}_3)_2 \cdot 6\text{H}_2\text{O}$ was dissolved in 100 mL of double distilled water. Then 40 mL cobalt nitrate solution was added to 40 mL copper nitrate solution the color was changed and 20 mL of leaf extract is added slightly to the solution and adjusted pH-9 with continuous stirring and after adjusting heating for 3 h at 70 °C. The precipitate was collected and light green color Co-doped copper oxide nanoparticles were obtained.



Similarly, 1% and 1.5% of cobalt-doped CuO nanomaterials were synthesized by following the same procedure. The as-synthesized CuO and cobalt-doped CuO NMs were kept for further characterization by UV-Vis, FTIR, XRD, SEM, and CV and antimicrobial studies [59, 64-65]

3.6. Characterization of CuO and Co-doped CuO nanomaterials

3.6.1. UV-Visible absorption spectroscopy analysis

UV-visible spectroscopy analysis of CuO and Co-doped CuO NMs were recorded on Shimadzu UV-240 nm (Shimadzu Corporation, Tokyo, Japan model noLF-204-LS) spectrometer. The UV-Visible spectra of the synthesized metal oxide nanoparticles was recorded around 200-800 nm. This spectrophotometer was used to analyze the unique optical properties and optical band gap which depends on the size and the shape of the nanoparticles. The analysis was accomplished at 25 °C using quartz cuvettes (1 cm optical path), and the distilled water is as a blank [65].

3.6.2. X-ray diffraction (XRD) analysis

The size and nature of copper oxide and Co-doped CuO NMs were determined by using the analysis XRD diffraction technique (X-ray diffraction; XPERT-PRO Machine) and at the setting of 30 kV/30 Ma Cu $k\alpha$ radian at 2θ . The scanning was done over a 2θ value range of 10° to 80° at 0.02 min^{-1} and at a 1-second time constant. The crystalline domain size was calculated using the Scherrer formula. $\lambda = 1.5406 \text{ \AA}$. Crystallite size is calculated using the Scherrer equation.

$$D = \frac{0.94\lambda}{\beta \cos\theta} \text{-----}3$$

Where D = Average crystallite size, λ = X-ray wavelength, β = Full width at half maxima (FWHM) of XRD spectral peak (in radians) and θ = Bragg's angle and k=Scherrer constant (the shape factor=0.94)

X-ray diffraction analysis with various nanoparticles has been studied by various research workers to find the high crystallinity of the prepared sample [66].

3.6.3. Fourier Transform Infrared [FTIR] spectroscopy analysis

For FTIR measurements, the precipitate of copper nanoparticles obtained using plant leaf extract of *kalanchoe petitiiana* is dried in an oven at 50 °C for 2 h. The dried synthesized copper oxide and Co-doped CuO nanoparticles were powdered and put on a sensor ready for analysis on an FTIR spectrophotometer in the diffuse reflectance mode operating at a resolution of 4 cm^{-1} . The dried CuO and Co-doped copper oxide nanoparticle was analyzed in the range of $400\text{-}4000 \text{ cm}^{-1}$ with an IR-2 Shimadzu spectrometer, using the sensor method [67].

3.6.4. Electrochemical analysis

The cyclic voltammetry characterization was done using a potentiostat with a three-electrode system. Drop Sense with inbuilt Drop view 200 software (Metrohm South Africa (Pty) Ltd., Johannesburg, South Africa) was fitted with screen printed carbon electrode (SPC) having an inner carbon working electrode (diameter of 4 mm), a silver pseudo-reference (Ag/AgCl) electrode (RE) and carbon counter electrode (CE). SPC was modified with CuO to obtain the modified working electrode used for the electrochemical studies. SPC electrode was modified by dropping about 0.5 μL of the ultrasonicated CuO nanoparticles samples on the surface of the electrode and air dried for 20 min. Noteworthy, the ultrasonication of the nanoparticles was done at room temperature. Each of the modified working electrodes was characterized using the $[\text{Fe}(\text{CN})_6]^{4-}/[\text{Fe}(\text{CN})_6]^{3-}$ (10 mM) redox probe in the presence of a phosphate buffer saline (PBS) (0.1 M, pH 7.0) supporting electrolyte. All cyclic voltammetry (CV) measurements were done at a scan rate of 50 mVs^{-1} over a potential window of -1.2 – $+1.2 \text{ V}$ [57].

3.6.4. Antimicrobial Activity analysis

In this study, two types of bacteria and fungus were obtained from the microbiology laboratory, biology department, Jimma University. The antimicrobial assays were done for Gram-negative *E. coli* and *S. typhi* and Gram-positive bacteria *S. aureus* and *B. cereus* and antifungal such as *C. albicans* tested by the agar disc diffusion method. Nutrient agar media was used to cultivate bacteria.

3.6.5. Preparation of inoculums

The test bacterial strains and fungus were transferred from the stock cultures as streaked on Nutrient Agar (NA) plates and incubated for 24 h. Well-separated bacterial colonies were used as inoculums. Bacteria were transferred using a bacteriological loop to autoclaved nutrient agar that is cooled to about $37 \text{ }^\circ\text{C}$ in a water bath mixed by gently swirling the flasks. The medium is then poured into sterile Petri plates, allowed to solidify, and used for the bio test. A fresh culture of inoculums of each culture was streaked on nutrient agar media in a Petri dish containing $100 \mu\text{g/ml}$ as-synthesized CuO and Co-doped CuO nanoparticles were impregnated using a micropipette on paper discs of 6 mm in diameter.

3.6.6. Preparation of test solutions

The samples were prepared for the bacterial test and labeled for *kalanchoe petitiiana* mediated CuO and Co-doped CuO nanoparticles. Zones of inhibition were measured after 24 h of incubation at 37 °C. The magnitude of antibacterial effect against, gram-negative *Escherichia coli*, *Salmonella typhi* and gram-positive bacteria *Staphylococcus aureus* and *Bacillus cereus* and also antifungal *C. albicans* was determined based on the inhibition zone measured in the disk diffusion test.

3.6.7. Disc diffusion method for antifungal activity

The antifungal activity of synthesized CuO and Co-doped copper oxide NMs was done using the standard disc diffusion method. The fungal strains used in the study are *Candida albicans*. The inoculums for the disc diffusion method were prepared using a suitable broth and the medium was dried at 37 °C before the application. The standardized inoculums are transferred into the sterilized Petri dish prepared earlier. The excess inoculums were removed by pressing and rotating the swab firmly against the side of the culture tube above the level of the liquid. The Petri dish was dried at room temperature for 24 h with lids closed. The Petri dish was divided into parts in which the samples were placed with the help of sterile forceps. DMSO solvent is used as a negative control. About 100 µg ml⁻¹ of standard Clitromazol was required to obtain a uniform way. The same amounts of copper oxide nanoparticles were prepared through a series of dilutions and approximately 100 µg ml⁻¹ was being used for evaluating its antifungal activity. Then Petri dishes were placed in the refrigerator at 4 °C or room temperature for 1 h for diffusion and incubated at 37 °C for 24 h. Finally, the zone of inhibition produced by different samples was measured using a standard scale [68].

4. RESULTS AND DISCUSSION

4.1. Phytochemical testing of the plant extracts

In this study, *kalanchoe petitiانا* has been extracted and then the presence of its phytochemicals, such as alkaloids, flavonoids, polyphenols, etc. was checked. Based on the results the naturally existing phytochemicals in the leaf extract were used as a reducing and capping agent during CuO and Co- doped CuO NMs synthesis. The results of qualitative phytochemical analysis of the *kalanchoe petitiانا* extract are shown in Figure 7 and Table 1 which revealed the presence of secondary metabolites such as alkaloids, polyphenols, flavonoids, etc. Therefore, the *kalanchoe petitiانا* leaf extract is composed of phytochemicals that are capable of reducing the Cu^{2+} ion by donating electrons, capping and stabilizing the formed nanoparticles

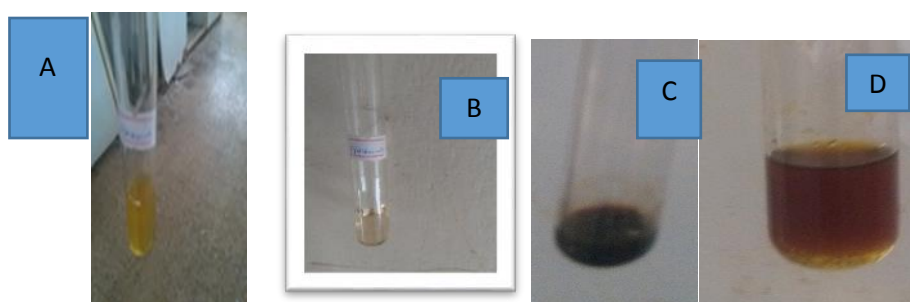


Figure 7. Phytochemical testing of plant extract

The color change was observed when the leaf extract of *kalanchoe petitiانا* was tested for the presence of (A) Flavonoids (a drop of NaOH) (B) flavonoids (a drop of dilute HCl) (C) phenols (D) Alkaloids

Table 1 Phytochemical analysis

S.N	Phytochemicals	chemical tests	observation	inference
1	Phenols	5 mL of leaf extract and a few drops of 5% neutral ferric chloride	Dark green	+
2	Flavonoids	20% of NaOH and a few drops of dilute HCl	yellow and colorless respectively	+
3	Alkaloids	0.5 g Iodide and 1.5 g potassium iodide	reddish brown precipitate	+

The functional groups of hydroxyl group (OH), and carbonyl (C=O) group act as reducing and stabilizing agents for the synthesis of nanomaterials. This result is in good agreement with the literature [69] in which it was tested for the presence of phytochemicals in Ocimum

lamiifolium (Damakese) plant extract. However, according to the [69] report alkaloid was not present in the extract but this study revealed the presence of alkaloids. This may be due to the type of solvent used during extraction, since different solvents can extract different families of Phytochemicals based on their polarity, hence varying the biological activity of the extracts [70].

4.3. Optimization of copper oxide nanomaterials

4.3.1. Optimization pH effects of CuO NMs

The pH is one of the factors that influence the size, shape, and composition of nanoparticles [62]. Further characterization was performed using UV–Vis spectrophotometry, which showed a distinct peak at 230 nm and it was in agreement with other studies on the green synthesis of CuO NMs using plant extract [71]. The surface Plasmon absorbance of copper colloids was obtained. The role of pH in the synthesized CuO NMs was carried out by altering the pH of *kalanchoe petitiiana* leaf extract. The difference in the intensity of the SPR peak ranged between 220-320 nm as shown in (Figure 8) the pH of obtained CuO NMs was found to be four variations in pH (5,7,9 and 11) [72]. Absorption in UV-visible spectra was the maximum at pH- 9. The increase in pH from 9 to 11 decreased the absorption. In acidic pH, nanoparticles aggregated out of the nucleation, while, at alkaline pH, great numbers of nuclei formed, instead of aggregation [29, 30]. So pH- 9 was found to be optimum to biosynthesize nanoparticles, which was in matched the values reported in the literature. Exhibited different SPR peaks as pH-9 (red peak) the SPR peak has higher absorbance at around 230 nm wavelength at maximum absorbance than the three peaks [63].

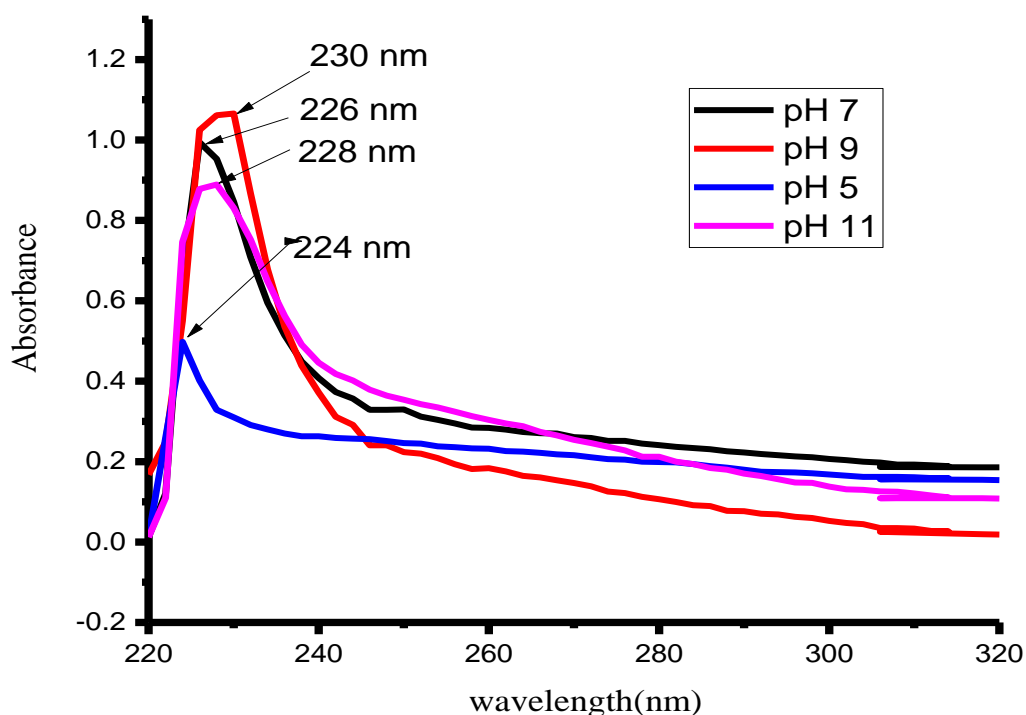


Figure 8. pH effects of CuO NMs

4.3.2. Optimization of precursor Concentration of Cu (NO₃)₂·3H₂O

The formation of copper oxide nanoparticles was studied by the variation of copper nitrate concentration from 0.05 to 0.15 M. The SPR absorption was increased due to increasing the concentration of copper ions from 0.05 to 0.1M (Appendix 3). This may be attributed to the formation of more CuONPs as the reaction progresses since the intensity of the surface Plasmon peak is directly proportional to the density of the CuONMs in the solution. As increasing in the concentration of copper nitrate more than 0.1 M the SPR absorbance decreased which could be due to the low number of reducing agent molecules. In the case of a low concentration (0.05 M) of copper nitrate, there is a low number of Cu²⁺ ions which have to be reduced to Cu nuclei [63].

4.3.3. Optimization of Plant extract

The formation of copper oxide nanoparticles depends on the ratio of extract Cu(NO₃)₂ (v/v). The UV-visible spectrum was recorded for the shift in SPR peaks position with variation in the amount of plant extract to precursor salt as shown in (Appendix 4). The maximum absorption was observed at 20 mL, but by increasing the volume to 30 mL, the absorption decreased and a broad peak was formed. The 20 mL was found to be typical to biosynthesize nanoparticles it showed maximum absorption at 238 nm [63].

4.3.4. Optimization Concentration of dopants

The absorption peak of Co-doped CuO NMs was also affected by the concentration of dopant [72]. To see the effect of the concentration of dopant (Co) on the absorption peak of CuO NPs; the dopant concentrations were varied as (0.5%, 1%, and 1.5%) while other parameters were kept constant and the absorbed wavelengths were 226, 228 and 231 nm while the concentration of dopant was increased from 0.5% to 1% the absorption peak was increased and while it was increased to 1.5% the absorption peak was decreased to 228 nm (Appendix 5) which resulted in a change in the optical band gap value. Co-doping was observed to reduce the band gap of NMs. This decrease in band gap may be attributed to the presence of impurity states between the CuO's conduction and valance bands due to Co-doping. As the number of dopant atoms increases, these impurity states coalesce near the conduction band's lowermost edges, reducing the gap between the conduction and valance bands. The result was in agreement with the reported literature [73].

4.4. Synthesis of CuO and Co-doped CuO nanomaterials

During the synthesis of CuO NPs, the color of the mixtures of leave extract and copper nitrate trihydrate solution was green at the beginning. After heating for 3 h with continuous stirring at 70 °C, a light green color was observed which indicates the formation of CuO NMs (Appendix 2a). Co-doped CuO NMs were synthesized in a similar way to CuO NMs but, with the addition of Co dopant and a deep green color was observed that indicates the formation of Co-doped CuO NMs (Appendix 2b). The copper and Co ions were reduced to their corresponding CuO NMs and Co-doped CuO NMs, and the synthesized nanoparticles were capped through phytochemicals present in plant extract [74].

4.5. Characterization of CuO and Co-doped CuO nanomaterials

4.5.1. Electrochemical analysis of CuO NMs

Electrochemical comparative studies of CuO were studied using cyclic voltammetry at a scan rate of 50 mV/s in 10 mM $[\text{Fe}(\text{CN})_6]^{4-}/[\text{Fe}(\text{CN})_6]^{3-}$ solution prepared in 0.1 M PBS. The screen print carbon electrode was modified with the CuO nanoparticles synthesized from the green method. The screen print electrodes were modified with the CuO nanoparticles and denoted as SPC/CuO, representing the green mediated CuO from water solvents (Figure 9). The voltammogram of the modified SPC electrodes of SPC/CuO showed redox peaks, an anodic peak at about 0.3 V, and cathodic peaks at a reduction potential of -0.25V for the $[\text{Fe}(\text{CN})_6]^{4-}/[\text{Fe}(\text{CN})_6]^{3-}$ probe. This result confirms that green synthesis enhances the electroactivity of the synthesized nanoparticles [56].

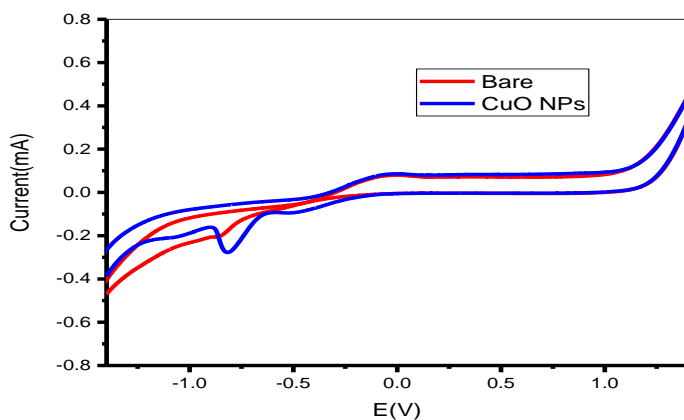


Figure 9. Cyclic voltammetry analysis

4.5.2. UV-Vis spectroscopy analysis of CuO NMs and Co-doped CuO NMs

UV-Visible absorption spectroscopy is an important tool to investigate the semiconducting nanoparticles for their optical properties. Absorption spectra of CuO and Co-doped CuO nanoparticles were taken using a UV-Visible spectrophotometer. Initially, the synthesized CuO and Co-doped CuO NMs were analyzed with a UV-Vis spectrophotometer between 220–320 nm scan range. These NPs showed a broad peak at the wavelength of CuO and Co-doped CuO nanoparticles are 230 and dopant 226, 228, and 231 nm respectively (Figure 10-13), corresponding to copper oxide and cobalt doped CuO NMs and these peaks were in agreement with the previously reported literature and from this, it was confirmed that the synthesized [63]. The values of the energy band gap (E_g of CuO and Co-doped CuO nanostructures were obtained from the optical diffuse reflectance spectra recorded at room temperature and shown in (Figures 10-13). The band-gap energy (E_g values were evaluated using the Tauc plot by the following equation

$$(\alpha h\nu)^2 = A(h\nu - E_g) \text{-----4}$$

Where A is a constant, that depends on the transition probability, α is an absorption coefficient, $h\nu$ is the photon incident energy, 2 is a constant that determines the type of optical transition and $n=2$ is a direct transition. The Tauc plot of CuO and $\text{Cu}_{1-x}\text{Co}_x\text{O}$ samples are shown in (Figure10-13).

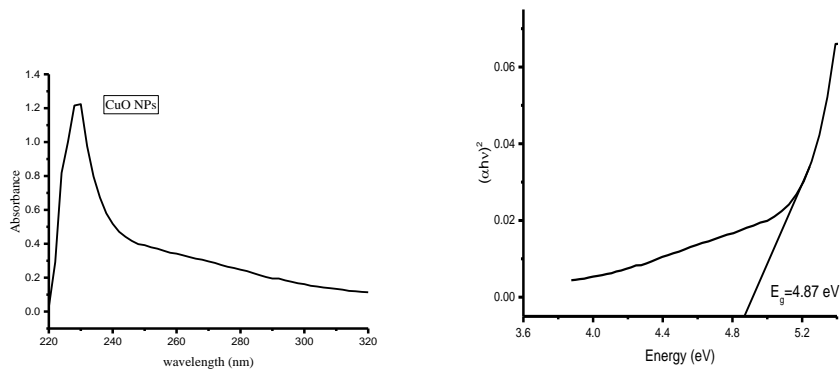


Figure 10 UV-Vis spectra of CuO NMs and energy band gap

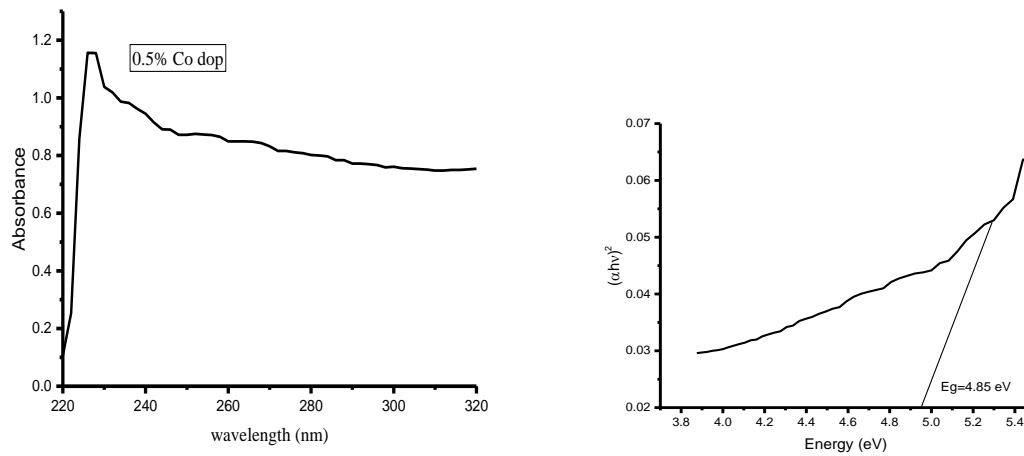


Figure 11 UV-Vis spectra of 0.5% Co doped CuO NPs and energy band gap

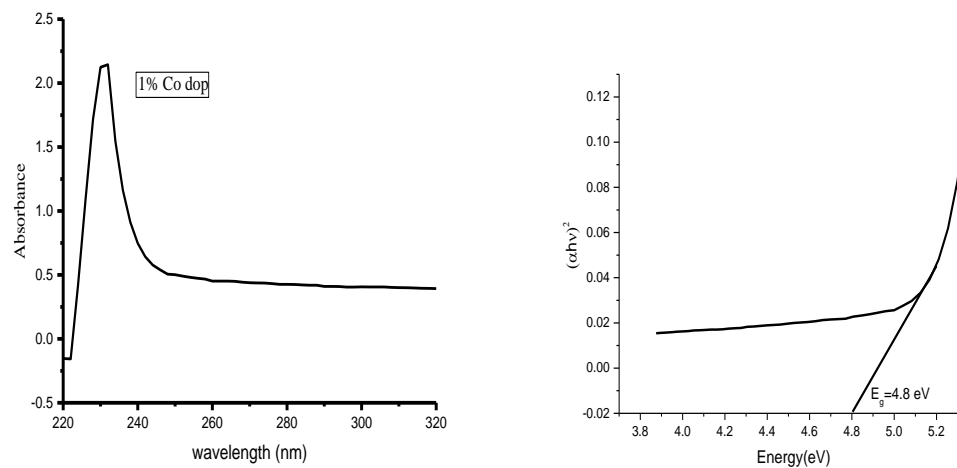


Figure 12 UV-Vis spectra of 1% Co doped CuO NPS and energy band gap

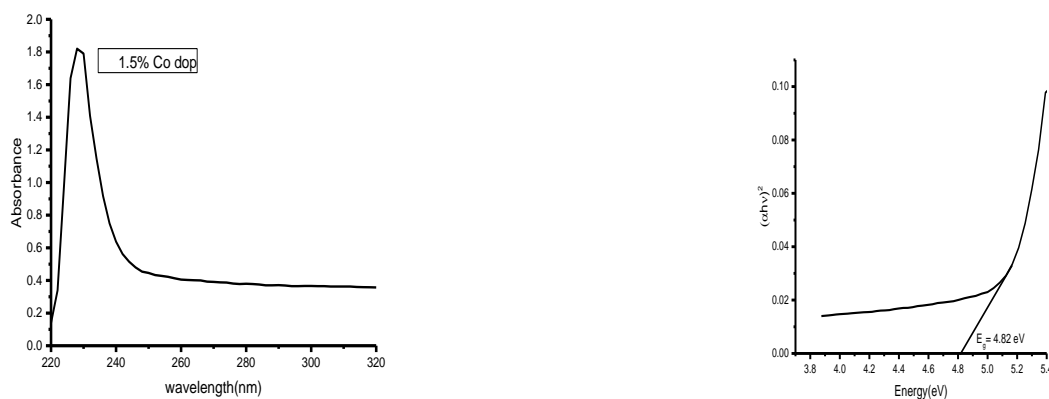


Figure 13 UV-Vis spectra of 1.5% Co-doped CuO NMs and energy band gap

For 0.5 and 1% doping of Co, the band gap has reduced to 4.85 and 4.8 eV respectively but when dopant concentration is increased to 1.5%, the band gap increases to 4.82 eV. The result was in close agreement with the reported literature [75]. The band gap of CuO nanoparticles is 4.87 eV which is higher than that of bulk CuO (1.85 eV) and the band gap of Co-doped CuO NPs 4.85, 4.8, and 4.82 eV. It has been observed that the band gap decreases with Co doping with the decrease in particle size. Intra gap defects have also been reported to decrease the band gap of CuO nanoparticles. They have observed that the intraband states are developed within the band gap due to the presence of dopants or valence defects (e.g. O vacancies and Cu^{1+} state) in CuO nanoparticles and these are the sources of decrease in the band gap. A similar decrease in the band gap of Ni-doped SnO_2 has also been observed, where the band gap decreases with Ni doping with the size reduction [76].

4.5.3. FTIR analysis of CuO and Co-doped CuO NMs

The dual role of the plant extract, as a reducing as well as capping agent, and the presence of some functional groups in both the *kalanchoe petitiiana* leaf extract and the synthesized CuO NPs and Co-doped CuO NMs were investigated by FT-IR analysis. FT-IR analysis was used to identify and get an approximate idea of the possible bio-molecules that are responsible for capping and stabilization of the CuO NPs and Co-doped CuO NMs with the leaf extract of *kalanchoe petitiiana*. As observed in (Figure 14 b). The major and strongest vibrational modes in the *kalanchoe petitiiana* leaf extract spectrum are those located at 3335, 2921, 2852, 1729, 1564, 1392, 1219, and 1013 cm^{-1} . A strong and broad peak at 3335 cm^{-1} can be attributed due to hydrogen-bonded O-H groups of alcohols and phenols and also due to the presence of amines N-H of amide. This agrees with the conclusion that leaf extract of *K.petitiiana* is composed of polyphenols, flavonoids, alkaloids, and other similar phytochemicals containing O-H and N-H bonds, which was Confirmed by using qualitative phytochemical analysis [77]. The bands at

2921 and 2852 cm^{-1} are assigned to C-H and CH_2 stretching mode in alkanes and the peak at 1729, 1564, 1392, 1219, and 1013 cm^{-1} represents hydroxyl (-OH) bending, C=O carbonyl group stretching, C=C aromatic ring, C-H or C-O stretching vibrations and stretching vibrations of C-N functional groups of amines, respectively. These peaks show the presence of phenolic compounds in the plant extract. This is in close agreement with the value reported in the literature [78, 79].

As observed in (Figure 14 a) the major and strongest vibrational modes FTIR spectrum of CuO NMs stabilized in *kalanchoe petitiانا* are those located at 3324, 2342, 1733, 1567, 1386, 1227, 1061, and 655 cm^{-1} . To identify the functional groups present in the sample, FT-IR analysis was performed which is denoted in (Figures 14 a and b). The peaks observed in the FTIR spectrum are responsible for the conversion of metal precursors into metal nanoparticles. The bands at 3334 cm^{-1} were responsible for the alcoholic O-H stretching, 2342 cm^{-1} and the broad peak represents the acidic O-H stretching. Moreover, the band at 1733 and 1387 cm^{-1} corresponded to the C=O and C-O stretching. The intense bands observed at 1227 cm^{-1} correspond to C-O-C stretch. [80]. The major M-O bands appeared at 655 cm^{-1} indicating the formation of the monoclinic phase of CuO NMs [81]. The absorption peak at 1061.0 cm^{-1} is the stretching vibration of the C-O group of primary and secondary alcohols [82].

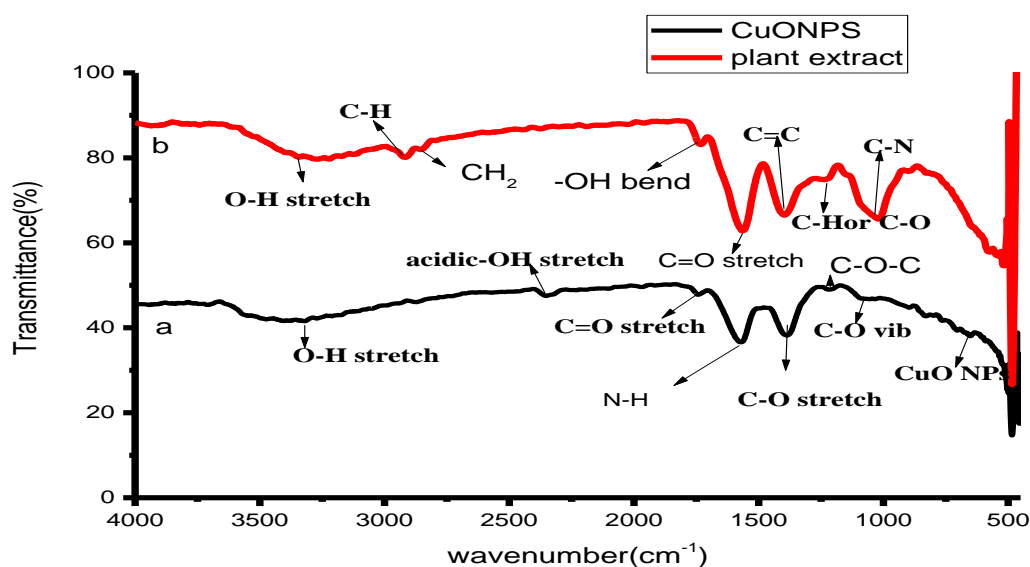


Figure 14. FTIR analysis of plant extract and CuO NMs

The FT-IR spectra were used to confirm the presence of functional group and plant metabolites, which were used for the reduction and stabilization of the green synthesized copper oxide nanoparticles and cobalt-doped copper oxide nanoparticles. In the FTIR spectrum, absorption bands at 558, 600, 620, 655, 1061, 1385, 1567, 1733, 3324, 3354, 3361 and

3381 cm^{-1} were present. Doping causes variation in intensity and position of the FTIR peaks which attributes to the fact that bond strength has been changed. It also confirms the successful doping of CuO host lattice. Absorption band around 558, 600, 620 and 655 cm^{-1} are indicates CuO and Co-doped CuO NMs. The peak at 1061 cm^{-1} is due to C-O stretching whereas 1567 cm^{-1} is related to C=O. The stretching band at 1733 cm^{-1} corresponds to the aldehyde or carbonyl groups. Peaks depicted around 3347, 3354, and 3361 cm^{-1} are related to the O-H stretching. Quite interestingly as the dopant concentration is increased, peak intensity is also enhanced [73]. The FT-IR spectra of the synthesized Copper oxide NPs (Figure 15) represent a broadband absorption peak at 3354 cm^{-1} indicating the stretching of O-H groups in water, and phenols [83]. However, after doping with Co reduction in intensity occurred and, this broadband of 0.5% disappeared. This may be related to the reduction of water content in the Co-doped CuO NMs or the interaction of the Co with the hydrogen-bonded O-H groups [84].

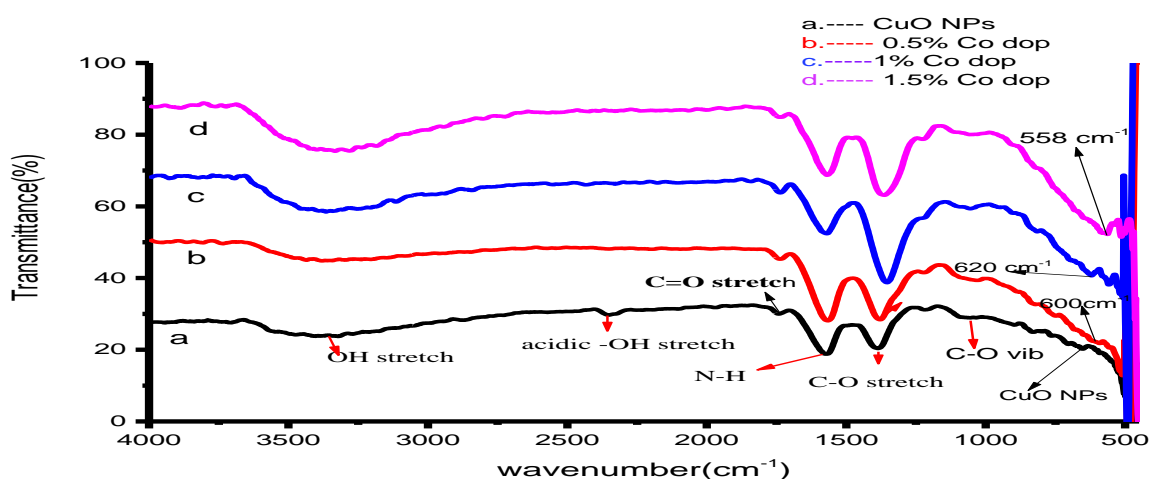


Figure 15. FTIR analysis of CuO and Co-doped CuO NMs

4.5.4. XRD analysis of CuO and Co-doped CuO NMs

An X-ray diffraction study was carried out on the prepared CuO NMs & Co-doped CuO NMs. The crystalline nature of nanoparticles was confirmed by the powder X-ray diffraction study and diffraction peaks are indexed in Figure 16. Represents the XRD pattern of green synthesized CuONMs. The specific diffraction peaks at $2\theta = 32.20^\circ, 35.70^\circ, 38.9^\circ, 48.95^\circ, 53.50^\circ, 58.50^\circ, 61.7^\circ, 66.3^\circ, 68.2^\circ, 72.5^\circ, \text{ and } 75.5^\circ$ were assigned to (100), (002), (200), (202), (020), (202), (113), (022), (020), (311), and (004) which were well crystal planes, respectively, which is in agreement with the previously reported work. The diffraction peaks in Figure. 12 indicate that the CuO has a monoclinic phase [85].

Table 2. XRD diffraction analysis of CuO and Co/CuO NPs

	2 θ (degree) CuO NPs XRD analysis										
Reported XRD analysis	32.49	35.5	38.4	48.8	53.4	58.22	61.5	66.24	67.98	72.36	75.7
observed	32.2	35.7	38.9	48.9	53.5	58.5	61.7	66.3	68.2	72.5	75.5
(hkl)	(100)	(002)	(200)	(202)	(020)	(202)	(113)	(022)	(020)	(311)	(004)

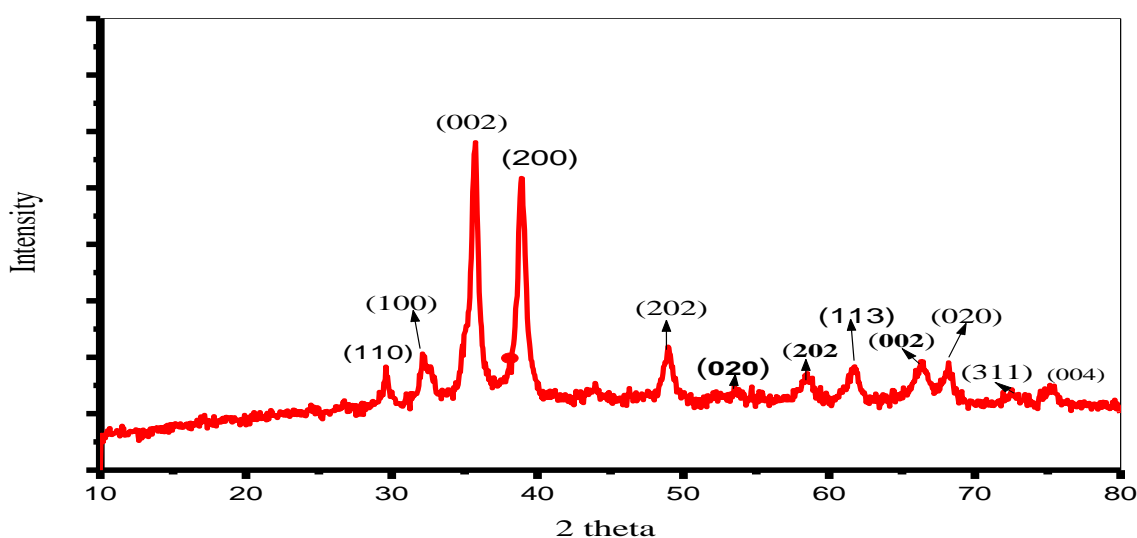


Figure 16. XRD analysis of CuO NMs

After doping CuO NMs with Co, the formation of minor extra peaks was observed in the XRD spectrum of Co-doped CuO NPs at $2\theta = 36.87^\circ$, 44.10° , 59° , and 76.46° related to the crystal planes (111), (200), (220), and (311) respectively. These additional peaks observed were peaks due to Co, and showed face centered cubic cobalt crystal (JCPDS No. 4- 0783). The green-synthesized CuO NMs were well-crystalline which was confirmed by the well-defined and high-intensity diffraction reflection peaks. The crystalline size (D) of the CuO NPs was calculated using Debye–Scherer's equation and the intensity of diffraction peaks decreases as the concentration of Co doping increases, indicating that the crystalline structure has deteriorated as a result of doping. The peak of cobalt oxide or cobalt hydroxide is absent in the XRD pattern. The concentration of Co caused a slight change in XRD peaks. A shift in the diffraction peak shows doping of the CuO lattice with Co ions. The Scherer equation was used to determine the crystallite size of the NMs, and the size of CuO and Co-doped CuO nanoparticles is shown to be decreased with the increasing concentration of Co dopant. The

decrease in NP crystallite size pure and Co (0.5 and 1%) doped CuO-NMs. due to the creation of Co–O–Cu bonds by Co doping [73].

Depending on the FWHM values at the preferred orientations (002) at $2\theta=35.7^\circ$, the samples crystallite size was evaluated using the Debye-Scherer formula

$$D = \frac{K\lambda}{\beta \cos\theta}$$

where D is the average crystalline size (Å), k is a constant 0.94, 'λ' is the wavelength of X-ray diffraction (0.1541nm), β is the angular line full width at half maximum (FWHM) intensity in radians, and 'θ' the Bragg's angle. The crystallite size of CuO NMs, and 0.5 %,1 %, and 1.5 % Co-doped CuO NMs prepared by using *kalanchoe petitiiana* leaf extract were 16.398 nm and 16.393 nm,16.386 nm,16.379 nm respectively. This result is in close agreement with the literature that reported crystal size of Co-doped CuO NMs was between 14-25 nm in the range [57]. With the increase in the dopant Co contents, the crystallite size decreases according to the lowering ionic radius of Co (0.079 nm and Cu (0.087 nm) [86].

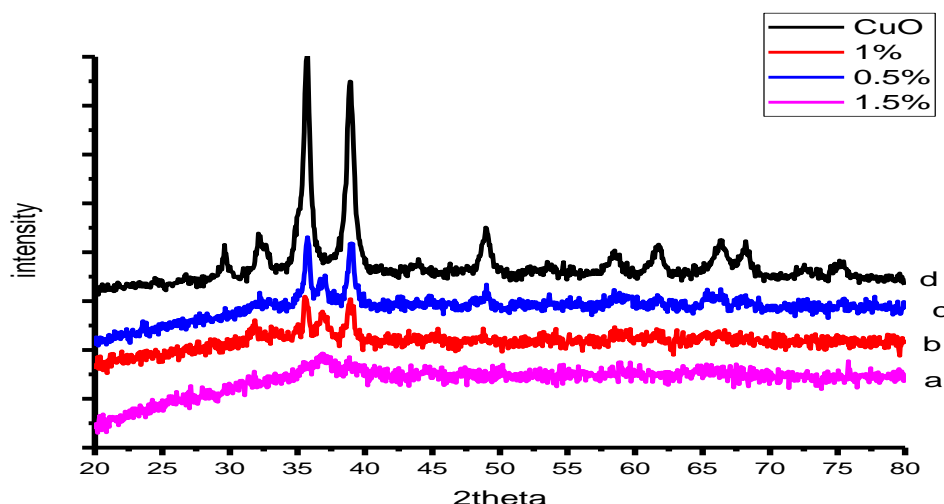


Figure 17. XRD CuO and Co-doped CuO NMs analysis

XRD graph of CuO and Co-doped CuO NMs a, b, c, and d indicates a 1.5%, 1%, and 0.5%, Co-doped CuO and CuO NMs respectively.

4.5.5. Scanning electron microscopic (SEM) analysis of CuO and Co-doped CuO NMs

Figure 18 (a and b) show the SEM images of the prepared CuO and Co-doped CuO nanoparticles. The image indicates that the CuO NMs show most synthesized nanoparticles are spherical (Figure 18 a). This result is in close relationship with recent findings [84, 87] literature that reported spherical CuO NMs. In the case of CuO NMs doped with Co (Figure 18 b), a mixture of spherical-shaped and rod-like structures was observed. The SEM images of

synthesized CuO NMs and Co-doped CuO NMs showed a rough surface that may be due to the encapsulation of plant extracts [87].

The formed CuO nanoparticles by using extract have dominantly spherical and circularly defined surface morphology as seen from the SEM micrographs in Figures 18 (a and b). Some rod-shaped nanoparticles have also survived. The formed CuO nanoparticles were split with diminutive space between them. The vast aggregation of CuO nanoparticles was avoided by the usage of plant extract in the synthesis. In some places, there was less aggregation of formed CuO nanoparticles was transpired. This phenomenon was ascribable to the overuse of extract [88].

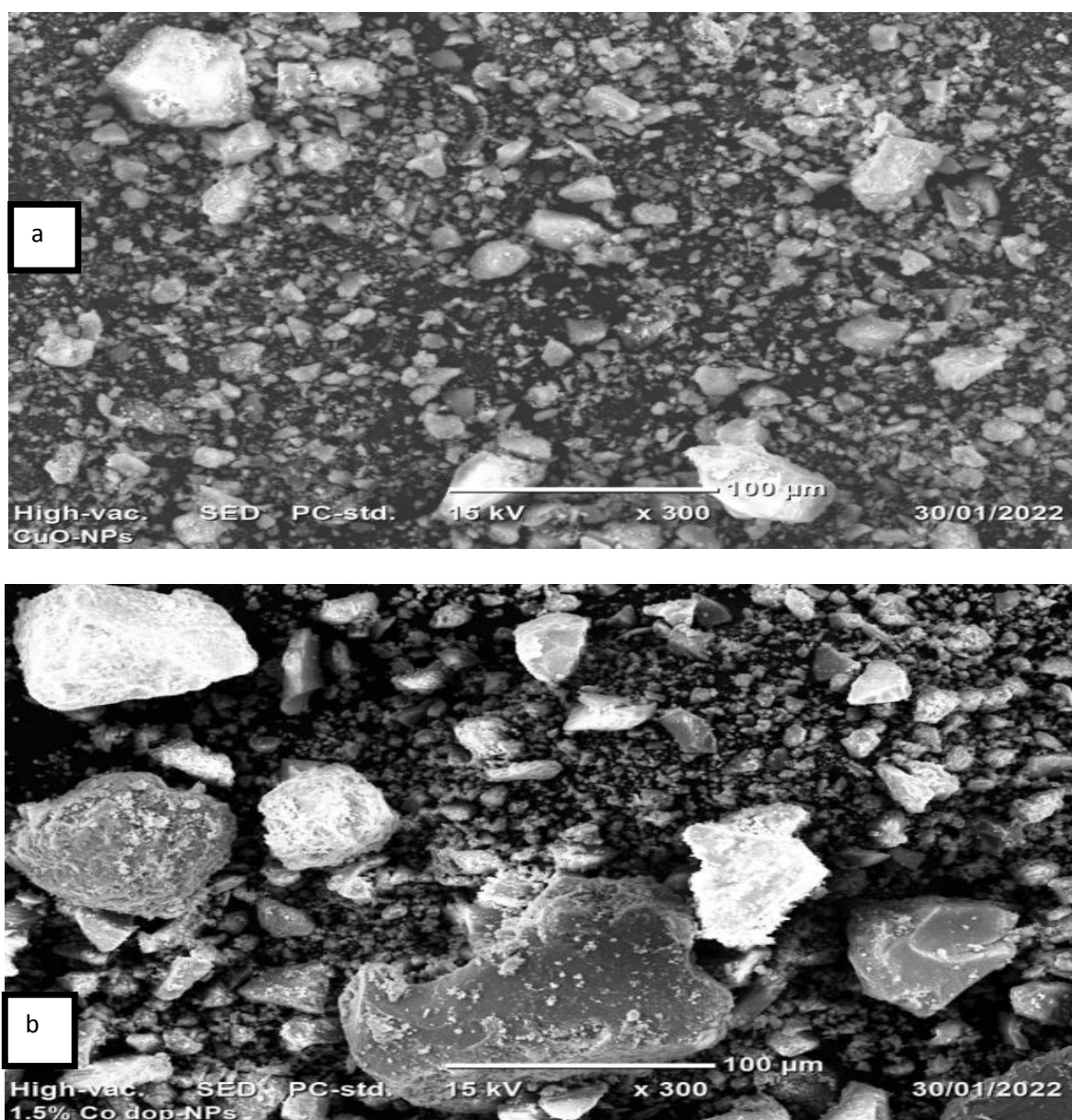


Figure 18. SEM analysis of a and b respectively CuO and Co-doped CuO NMs

4.6. Antimicrobial activity

4.6.1. Antibacterial activity

The results of the antimicrobial test were shown in tables 2 and 3.

Effect of CuO and Co-doped CuO NMs on selected bacteria (*Salmonella typhi*, *Bacillus cereus*, *Staphylococcus aureus*, and *Escherichia coli* at 100 μ g/ml concentrations.

In vitro antibacterial activity of CuO and cobalt-doped CuO NPs using some human pathogenic bacteria by disc diffusion methods.

Table 3. Antibacterial test results

B.Strain	zone of inhibition in mm						
	+tve control/gentamicin	-ve control/DMSO	CuO NPs	0.5% Co dop	1% Co dop	1.5% Co dop	PE
B.Cereus	20.5 mm	-	20	19.5	21.5	22.5	-
S.aures	21 mm	-	24	23	26	28	-
E.coli	22 mm	-	19	20	20.5	23.5	-
S.typhi	21.5 mm	-	25	23.5	25.5	28.5	-

(-) indicates = No inhibition zone, PE= plant extract

In the present study, the antibacterial activity of the synthesized copper oxide and Co-doped CuO nanoparticles using *kalanchoe petitiiana* leaf extract was examined against both two Gram-negative (*E. coli* and *S.typhi*) and two Gram-positive (*S. aureus* and *B.Cereus*) bacteria by disc diffusion test. The zone of inhibition (ZOI) values for the above-mentioned samples was recorded in (Table 3). The negative control (DMSO) and plant extract were not shown any activity against the bacterial strains tested. On the contrary, antibacterial activity was observed against pathogens when CuO NMs and Co-doped CuO NMs used. The antibacterial effect of CuONMs and Co-doped CuO NMs against all four bacteria compared with control, the diameter of ZOI in mm varied for all the tested bacteria at the same concentration level of CuONMs and Co-doped CuO NMs. It is seen that the growth of Gram-negative bacterial strains, *Salmonella typhi* was more effectively affected by CuO NMs than that of the Gram-positive strains *Staphylococcus aureus* and *Bacillus cereus* at 100 μ g/ml. The difference in activity between these two types of bacteria could be attributed to the structural and compositional differences in the cell membrane. The CuO NMs and Co dope CuO NMs showed good antibacterial activity against *salmonella typhi*, *S. aureus*, *Escherichia coli*, and *Bacillus cereus* with a maximum inhibition zone of 25, 24, 19, and 20 mm, respectively. The ZOI of the

copper oxide and Co-doped CuO nanoparticles is higher when it is tested against *S.typhi* than when tested against *S.aures*, *E. coli*, and *B. cereus*. These results refer to differences in the cell wall of each strain; the cell wall of Gram-negative strains (*S.typhi* are wider than the cell wall of Gram-positive strains (*S. aureus*). This is probably of the toxicity of copper oxide and Co-doped CuO ions on include a rapid DNA degradation, followed by a reduction of bacterial respiration; it is also known that copper oxide ions inhibit certain cytochromes in the membrane.

The results revealed that the bacterial sensitivity to nanoparticles was found to vary depending on the microbial species. Gram-positive bacteria have thicker peptidoglycan cell membranes compared to the Gram-negative bacteria and it is harder for CuO to penetrate, resulting in a low antibacterial response [89]. In addition, the damage to the cell membrane might directly lead to the leakage of minerals, proteins, lipids, and genetic materials causing ultimate cell death. Furthermore, the antibacterial activity increases with a decrease in particle size, due to the higher surface area of the samples [90].

The antibacterial test results showed that *S. aureus* is less susceptible to CuO NMs when compared to *S. typhi* which is in agreement with the results reported in the literature [89]. Obtained experimental results have shown that synthesized CuO NMs have antibacterial activity on both gram-positive and negative bacteria. CuO NMS was more sensitive to gram-positive bacteria (*aureus*) and gram-negative bacteria (*S. typhi*) and also Co-doped copper oxide nanoparticles zone of inhibition were increased from 0.5% to 1.5% Co doping NMs. The antibacterial effect of CuO and Co-doped CuO nanoparticles is due to the generation of reactive oxygen species, which cause bacterial cell damage [90, 91].

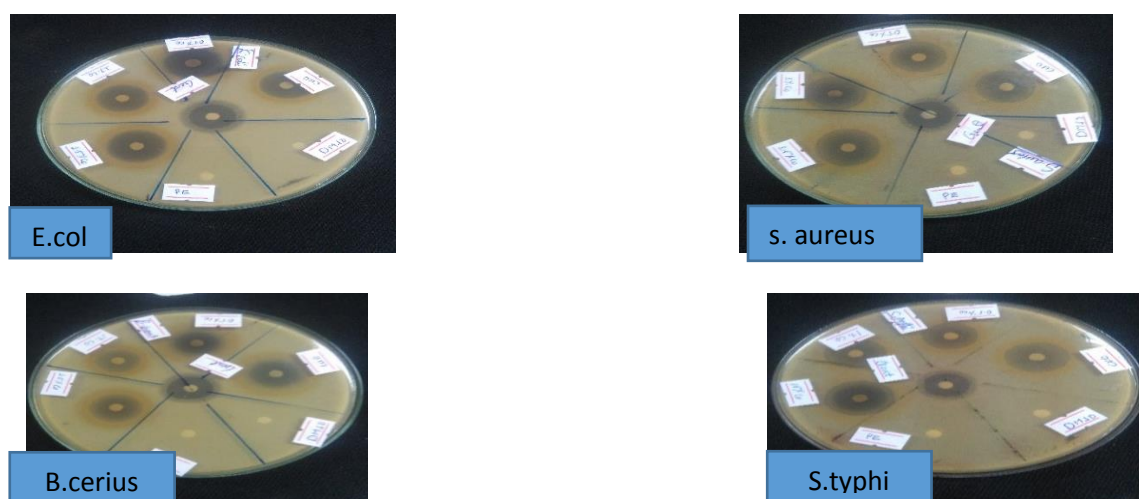


Figure 19. Zone of antibacterial activity

4.6.2. Antifungal activity

Table 4 . Antifungal test results

fungus Strains	zone of inhibition in mm						
	+ve control/Clitromazo l	-ve control/DM SO	CuO NMs	0.5%Co dop	1% Co dop	1.5% Co dop	PE
C. albicans	16mm	-	20mm	20.5 mm	22 mm	24 mm	-

(-) indicates= No inhibition

PE = Plant extract

In general copper oxide, NMs and Co-doped CuO NMs are effective against a wide range of pathogens. The antifungal activity was measured by the disc diffusion method using fungi stains such as *Candida albicans*. Clotrimazole was kept as the standard and the zone of inhibition was noted. Copper oxide and Co-doped copper oxide nanoparticles showed a clear zone of inhibition as indicated in Table 4 against *Candida albicans*. It is reported that CuO nanoparticles attach to the surface of the cell membrane, disturb its function and penetrate directly with the fungus's outer membrane and release CuO ions. Clotrimazol 100µg/ml was used as control. The studies conform with the green synthesis of copper oxide nanoparticles using a natural reducer and stabilizer and after an evaluation of antifungal activity (Table 4), it is inferred that the synthesized copper oxide NMs and Co-doped CuO NMs show a better antifungal activity. The size and concentration of the copper oxide nanoparticles play a vital role in exhibiting antimicrobial activity [92].

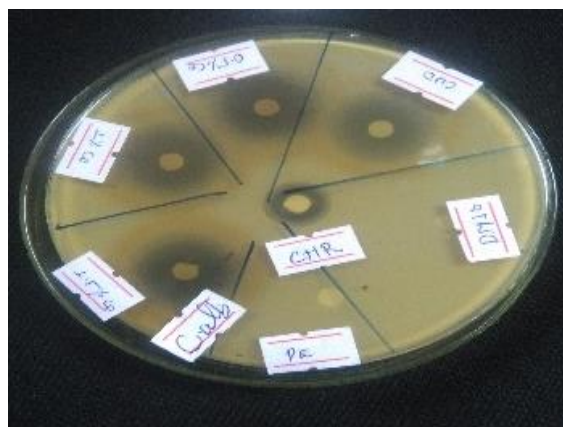


Figure 20. Zone of inhibition antifungal activity

5. CONCLUSION AND RECOMMENDATION

5.1. Conclusion

To summarize the reported work, a simple green method has been used for the preparation of CuO and Co-doped CuO NMs. A simple, clean, economically viable, and green approach has been established for the synthesized CuO NMs by using the nontoxic, cheap, and easily available leaf of *Kalanchoe petitiiana* as a reducing and capping agent without using any harsh, synthetic reducing agents. The green synthesis of CuO NMs and Co-doped CuO NMs found to be eco-friendly since the reactions involve exudates from plant extracts. The UV-Vis absorption peak at 230 nm and 228 nm indicates the synthesis of CuO and Co-doped CuO NMs. The powdered XRD patterns of the samples showed that the synthesized materials belonged to the monoclinic crystal system and its average crystallite size was found to be in the nanometer range. XRD pattern showed distinctive peaks corresponding to (002) and (111) planes that can be indexed as the typical monoclinic structure. The functional groups were identified by FTIR spectra. The optical study reveals that the energy band gap of synthesized nanoparticles shows enhancement results towards optical properties. The Co-doping further results in the absorption of the peak in the visible region area and successfully enhances the ability to absorb visible light that arises on account of the d-d transition involved between closely spaced Co^{2+} and Cu^{2+} ions. The observed band gap of pure CuO NMs and 1% Co-doped CuO NMs are 4.87 and 4.8 eV, respectively and the reduction of the band gap is because of particle size reduction and quantum confinement effect.

The designed CuO and Co-doped CuO NMs are highly stable and shown significant antibacterial activity against these bacterial strains with a maximum inhibition zone of 25, and 24 mm in *S.typhi*, and *S. aureus* respectively, and a minimum inhibition zone of 19 mm in *E.coli* and also Co-doping CuO NMs increasing ZOI. Antifungal testing inhibition zone is 20 mm and co-doping 21, 21, and 22 mm respectively. From the technological point of view, these obtained Copper oxide and Co-doped copper oxide nanomaterials have potential applications in the biomedical field and this simple procedure has several advantages such as cost-effectiveness, and compatibility for medical and pharmaceutical applications as well as large scale commercial production.

5.2. Recommendation

As the result of the rising concern for the environment due to the rising emission of toxic gases and materials that are brought about by technology in itself. The green synthesis of nanoparticles not only CuO nanoparticles has proven to be best budget-friendly and nontoxic. Therefore the government or other science inclined companies can take this up as a project to develop nanoparticles that serve the purpose of most indispensable toxic material emitting machines today, thus bringing about a safer environment but at the same time not hindering technological advancement.

The advance study should be carried out on proper isolation and characterization of compounds acting as the reducing agents in each plant extract which were not addressed by this study. Furthermore, the antimicrobial activities of the CuO nanomaterials should also be tested on other microbial species which were not addressed by this study.

6. REFERENCE

1. Naveen, A.Th.; Kumarb, K.; Kumar, K. Sh.Application of Co-doped copper oxide nanoparticles against different multidrug resistance bacteria. *Inorganic and Nano-Metal Chemistry*, **2020**, DOI: 10.1080/24701556.1728554
2. Sundaramurthy, N.; Parthian, C. Biosynthesis of copper oxide nanoparticles using pyrus pyrifolia leaf extract and evolve the catalytic activity. *Int. Research J, of Engineering and Technology (IRJET)*. **2015**, Volume: 02 Issue: 06.
3. Salem, S.S.; Fouad, M.M.G.; Fouad, A.; Awad, M.A.; Al-Olayan, E.M.; Allam, A.A.; Shaheen, T.I. Antibacterial, Cytotoxicity and Larvicidal Activity of Green Synthesized Selenium Nanoparticles Using Penicillium corylophilum. *Journal of Cluster Science* **2021**, 32, 351-361, DOI:10.1007/s10876-020-01794-8.
4. Elfeky, A.S.; Salem, S.S.; Elzaref, A.S.; Owda, M.E.; Eladawy, H.A.; Saeed, A.M.; Awad, M.A.; AbouZeid, R.E.; Fouda, A. Multifunctional cellulose nanocrystal /metal oxide hybrid, photo-degradation, antibacterial and larvicidal activities. *Carbohydrate Polymers* **2020**, 230, 115711, DOI:https://DOI.org/10.1016/j.carbpol.2019.115711.
5. Abdelmoneim, H.E.M.; Wassel, M.A.; Elfeky, A.S.; Bendary, S.H.; Awad, M.A.; Salem, S.S.; Mahmoud, S.A. Multiple Applications of CdS/TiO₂ Nanocomposites Synthesized via Microwave-Assisted Sol–Gel. *Journal of Cluster Science* **2021**, 10.1007/s10876-021-02041-4, DOI: 10.1007/s10876-021-02041-4.
6. Alsharif, S.M.; Salem, S.S.; Abdel-Rahman, M.A.; Fouda, A.; Eid, A.M.; El-Din Hassan, S.; Awad, M.A.; Mohamed, A.A. Multifunctional properties of spherical silver nanoparticles fabricated by different microbial taxa. *Heliyon* **2020**, 6, DOI:10.1016/j.heliyon.2020.e03943.
7. Eid, A.M.; Fouda, A.; Niedbała, G.; Hassan, S.E.D.; Salem, S.S.; Abdo, A.M.; Hetta, H.F.; Shaheen, T.I. Endophytic streptomyces laurentii mediated green synthesis of Ag-NPs with antibacterial and anticancer properties for developing functional textile fabric properties. *Antibiotics* **2020**, 9, 1-18, DOI: 10.3390/antibiotics9100641.
8. Mohamed, A.A.; Fouda, A.; Abdel-Rahman, M.A.; Hassan, S.E.D.; El-Gamal, M.S.; Salem, S.S.; Shaheen, T.I. Fungal strain impacts the shape, bioactivity, and multifunctional properties of green synthesized zinc oxide nanoparticles. *Biocatalysis and Agricultural Biotechnology* **2019**, 19, DOI:10.1016/j.bcab.2019.101103.
9. Sharaf, O.M.; Al-Gamal, M.S.; Ibrahim, G.A.; Dabiza, N.M.; Salem, S.S.; El-ssayad, M.F.; Youssef, A.M. Evaluation and characterization of some protective culture metabolites in free

- and nano-chitosan-loaded forms against common contaminants of Egyptian cheese. *Carbohydrate Polymers* **2019**, 223, 115094, DOI: <https://doi.org/10.1016/>.
10. Kaur, M. Impact of Response Surface Methodology Optimized Synthesis Parameters on In vitro Anti-inflammatory Activity of Iron Nanoparticles Synthesized using *Ocimum tenuiflorum* Linn. *BioNanoScience* **2020**, 10, 1-10, DOI: 10.1007/s12668-019-00681-5.
 11. Karunakaran, G.; Jagathambal, M.; Gusev, A.; Torres, J.A.L.; Kolesnikov, E.; Kuznetsov, D. Rapid Biosynthesis of AgNPs Using Soil Bacterium *Azotobacter vinelandii* With Promising Antioxidant and Antibacterial Activities for Biomedical Applications. *JOM* **2017**, 69, 1206-1212, DOI:10.1007/s11837-016-2175-8.
 12. Rabiee, N.; Bagherzadeh, M.; Kiani, M.; Mohammed, A. G.; Etesamifar, F.; Hossein, A. Jshakeri, A. Biosynthesis of Copper Oxide Nanoparticles with Potential Biomedical Applications. *Int J of Nanomedicine*. **2020**, 15, 3983–3999
 13. Alavil, M.; Dehestaniathar, S.; Mohammadi, Sh.; Makeki, A.; Karimi, N. Antibacterial Activities of Phytofabricated ZnO and CuO NPs by *Mentha pulegium* Leaf/Flower Mixture Extract against Antibiotic-Resistant Bacteria. *Adv Pharm Bull*, **2021**, 11(3), 497-504 DOI: 10.34172/apb.2021.057.
 14. Amin, F.; Khattak, B.; Alotaibi, Amal A.; Qasim, M.; Ahamd, I.; Ullah, R.; Bouriha, M.; Gul, A.; Zahoor, S.; Ahmad, R. Green Synthesis of Copper Oxide Nanoparticles Using *Aerva javanica* Leaf Extract and Their Characterization and Investigation of In Vitro Antimicrobial Potential and Cytotoxic Activities. *Evidence-Based Complementary and Alternative Medicine*, **2021**, Volume 12, 5589703, <https://doi.org/10.1155/2021/5589703>.
 15. Cimen, B.; Sengu, S.; Ergut, M.; Ozer, A. Green Synthesis and Characterization of CuO Nanoparticles: Telon Blue AGLF and Methylene Blue Adsorption. *Sinop Uni J Nat Sci*. **2019**, 4 (1): 1-20
 16. Yamini, G.; Sudha, L.; Fouzia, B.; Ezhilarasan, A. S. Green synthesis of silver nanoparticles from *Cleome viscosa*: synthesis and antimicrobial activity. *IPCBE IACSIT Press, Singapore*, **2011**, pp. 334-337.
 17. Ahmed, Y.; Hussain, J.; Ullah, F.; Asif, S. Green synthesis of copper oxide and cobalt oxide nanoparticles using *Spinacia oleracea* leaf extract.

18. Mohamed, N.; Judith. J. V.; John.L. K.; Bououdina. M. B and Hussain. Sh. Optical and Magnetic Properties of Co-Doped CuO Flower/Plates/Particles-Like Nanostructures. *J. Nanoscience and Nanotechnology*.**2014**, Vol. 14, 2577–2583.
19. Huang, J.; Li, Q.;Sun, D.; Lu, Y.; Su, Y.;Yang, X.; Wang, H.; Wang, Y.; Shao, W.; He, N.; Hang, N.J. Biosynthesis of silver and gold nanoparticles by novel sundried Cinnamomum camphora leaf. *Nanotechnology*. **2007**, 18(10), 105104-105115. 46–2353
20. Ledwith, D.M.; Whelan, A.M.; Kelly, J.M. A rapid, straightforward method for controlling the morphology of stable silver nanoparticles. *J. of Materials Chemistry*. **2007**, 17(23):2459.
21. Shankar, S.S.; Rai, A.; Ahmad, A.; Sastry, M. Controlling the Optical Properties of Lemongrass Extract Synthesized Gold Nanotriangles and Potential Application in Infrared Absorbing Optical Coatings. *Chemistry of Materials*. **2005**, 17(3), 566-72.
22. Dina, A. A .; Mohamed. A .; Mohamed, I.; Hashem. A.; Magda .A. A. Antibacterial Activity of Ecofriendly Biologically Synthesized Copper Oxide Nanoparticles. *Egypt. J. Chem.***2021**, Vol. 64, No. 8 pp. 4099 – 4104.
23. Nair, R.; Varghese, S.H.; Nair, B.G.; Maekawa, T.; Yoshida, Y.; Kumar, S.D. Nanoparticulate material delivery to plants, *Plant Science*.**2010**, 179, 154–163.
24. Hodes, G. When small is different: Some recent advances in concept and app.**2007**
25. Uskokovic, V. Nanomaterials, and Nanotechnologies: Approaching the crest of this big wave. *Current Nanoscience*.**2008**, 4, 119-129.
26. Goyer, R. A. Which Metals are Essential for Human Health? *Int.Council on Metals and the Environment Newsletter*. **1997**, 5 (2): 5.
27. Abou, E.N.; Eftaiha A.A .; Warthan, A. A .; Ammar, R.A.A. Synthesis and applications of silver nanoparticles. *Arabian J. of Chemistry*. **2010**. 3 (3):135-40.
28. Krithiga, N.; Jayachitra, A.; Raja, L. Synthesis, characterization and analysis of the effect of copper oxide nanoparticles in biological systems, *An Indian Journal of NanoScience*.**2013**, 1(1), 6-15.
29. Burda, C.X.; Chen, R. Narayanan and M.A. El-Sayed. Chemistry and properties of nanocrystals of different shapes. *Chem. Rev.***2005**, 10, 1025–1102.

30. van Dijken, A.; Meulenkamp, E.A.; Vanmaekelbergh, D.; Meijerink, A. Identification of the transition responsible for the visible emission in ZnO using quantum size effects. *Journal of Luminescence*. **2000**; *90* (3-4):123-8.
31. Parasharu, K.; S.a.S.A. Bio inspired Synthesis of Silver Nanoparticles" Digest. *Journal of Nanomaterials and Biostructures*. **2009**, *4*:p.159-166.
32. Begum, N.A.; M.S.a.B.L.R.A. "Mondal Colloids and Surface B" Biointerfaces, **2009**. *71*: p.113-118.
33. Mohammed .A.; Shafey. El. Green synthesis of metal and metal oxide nanoparticles from plant leaf extracts and their applications: A review Green Processing and Synthesis. **2020**; *9*, 304–339
34. Hsieh, Y .J.; Leu, Y.L.; Chang, C.J. The anticancer activity of Kalanchoe tubiflora. *Alt Med*. **2013**, *1*, 18- 19.
35. Abebe, D. Medicinal plants and other useful plants of Ethiopia. Ethiopian Health and Nutrition Institution, Addis Abeba. **2003**, 205-218
36. Maini.A.;shah. M.A. Investigation on Physical properties of Nanosized Copper oxide (CuO) doped with Cobalt (Co): A material for electronic device application. *International Journal of Ceramic Engineering & Science*.**2021**,DOI:10.1002/ces2.10097
- 37.Srivastava's .; Agarwalb, A. influence of Co doping on structural and optical properties of CuO nanoparticles. *J. of Ovonic Research*, **2018**, Vol. 14, No. 5, p. 395 – 404
38. Enrolment, A. Synthesis, Characterization and Antibacterial Study of co-doped Copper Oxide Nanoparticles. *Department of Physics, School of Basic and App. Sciences*,**2018**, p 1-15
39. Khmissi, H.; Sayed, E.A.; Shaban, M. Structural, morphological, optical properties and wettability of spin-coated copper oxide; influences of film thickness, Ni, and (La, Ni) Co-doping. *Mater. Sci*.**2016**,*51* (12):5924-38.
40. Warisa,A.;Dina,M.;Ali,A.; Ali, M.; Afridia, Sh.; Baset, A. .; Ullah. A.K. A Review of Green Synthesis of Copper Oxide Nanoparticles and Their Diverse Biomedical Applications. *Inor.ChemistryCommunications*,**2020**,DOI:<https://DOI.org/10.1016/j.inoche>
41. Warisa, A.;Din, M.;Ali, A.; Ali, M.; Afridi, Sh.; Baset, A. .; Ullah,A. K. A comprehensive review of green synthesis of copper oxide nanoparticles and their diverse biomedical applications. *Inorganic Chemistry Communications*, **2021**,*123*, 108369

42. Ismail, N. A .; Shameli, K .; Che, J.N W .; Rasit, R. A.; Mohamad, S .S .; Mohamed, E.I. Preparation of Copper Nanoparticles by Green Biosynthesis Method: A Short Review. *Materials Science and Engineering*.**2021**, DOI:10.1088/1757-899X/1051/1/012084
43. Chakraborty.; Banerjee.; Chakraborty, P.; Banerjee, A.; Chanda, S.; Ray, K, Archarya, K.; Sarkar, J. Green synthesis of copper/copper oxide nanoparticles and their applications. A review, *Green Chemistry Letters and Reviews*, **2022**,185-213, DOI: 10.1080/17518253.2022.2025916
44. Rakibul, M. I.;Saiduzzaman, M.; Shahriyar, S.N.; Kabir,A, A, A.; Farhad, S.F.U. Synthesis, characterization and visible light-responsive photocatalysis properties of Ce doped CuO nanoparticles: A combined experimental and DFT+U study. *Colloids and Surfaces A: Physicochemical and Engineering Aspects*, **2021**, 617, 126386.
45. Nagajyothi, P.C.; Lee, K.D. Synthesis of Plant-Mediated Silver Nanoparticles Using Dioscorea batatas Rhizome Extract and Evaluation of Their Antimicrobial Activities. *Journal of Nanomaterials*.**2011**, 573429.
46. Ahmad, N.; Sharma, S.; Singh, V. N.; Shamsi, S. F .; Fatma, A .; Mehta, B. R. Biosynthesis of Silver Nanoparticles from Desmodium triflorum: A novel approach towards weed utilization. *Biotechnology Research International Volume*.**2011**
47. Valodkar, M.; Rathore, P. S.; Jadeja, R. N.; Thounaojam, M.; Devkar, R.V.; Thakore, S. Cytotoxicity evaluation and antimicrobial studies of starch capped water-soluble copper nanoparticles. *J. Hazard. Mater.***2012**, 201–202,244–49.
48. Devanthiran.; Sophia. P. M. S .; Suriani. I.; Noor. H. N.; N. M.A. Plant-Based Biosynthesis of Copper/Copper Oxide Nanoparticles: An Update on Their Applications in Biomedicine, Mechanisms, and Toxicity.**2021**, 11, 564
49. Adewale, S.A .; Similoluwa, A.F.; Adekunle, F.F .; Kolawole, A.O. Green synthesis of copper oxide nanoparticles for biomedical application and environmental remediation. *Review article Heliyon* 6, **2020**, p 1-12 e04508.
50. Park, Y.; Hong, Y.; Weyers, A.; Kim, Y.; Linhardt, R. Polysaccharides and phytochemicals: A natural reservoir for the green synthesis of gold and silver nanoparticles. *IET Nanobiotechnol.* **2011**, 5, 69–78. [CrossRef].
51. Fazlzadeh, M.; Rahmani, K.; Zarei, A.; Abdoallahzadeh, H.; Nasiri, F.; Khosravi, R. A novel green synthesis of zero-valent iron nanoparticles (NZVI) using three plant extracts and

- their efficient application for removal of Cr (VI) from aqueous solutions. *Adv. Powder Technol.* **2017**, 28, 122–130. [CrossRef].
52. Berra, D.; Laouini, S.; Benhaoua, B.; Ouahrani, M.; Berrani, D.; Rahal, A. Green synthesis of copper oxide nanoparticles by Pheonix dactylifera L leaves extract. *Digest J. Nanomater. Biostruct.* **2018**, 13, 1231–1238.
53. Mary, A.A.; Ansari, A.T.; Subramanian, R. Sugarcane juice mediated synthesis of copper oxide nanoparticles, characterization, and their antibacterial activity. *J. King Saud Univ. Sci.* **2019**, 31, 1103–1114.
54. Asemani, M.; Anarjan, N. Green synthesis of copper oxide nanoparticles using Juglans regia leaf extract and assessment of their physicochemical and biological properties. *Green Process. Synth.* **2019**, 8, 557–567.
55. Akintelu, S.A.; Folorunso, A.S.; Folorunso, F.A.; Oyebamiji, A.K. Green synthesis of copper oxide nanoparticles for biomedical application and environmental remediation. *Heliyon* **2020**, 6, e04508.
56. Sackey, J.; Nwanya, A.; Bashir, A.; Matinise, N.; Ngilirabanga, J.; Ameh, A.; Coetsee, E.; Maaza, M. Electrochemical properties of Euphorbia pulcherrima mediated copper oxide nanoparticles. *Mater. Chem. Phys.* **2020**, 244, 122714
57. Obakeng, P. K.; Adeyemi, O. A.; Saheed, E. E.; Omolola, E. F. Green and Traditional Synthesis of Copper Oxide Nanoparticles Comparative Study. *Nanomaterials* **2020**, 10, 2502; DOI: 10.3390/nano10122502
58. Jitendra, M.; Amla, B.; Abhijeet, S.; Madan, M.S. Phytofabrication of nanoparticles through the plant as nanofactories. *Adv. Natural Sci. Nanosci. Nanotechnol.* **2014**, 5 10.
59. Narasaiah. P.; Mandal. B .K.; Sarada. N. C. Biosynthesis of Copper Oxide nanoparticles from Drypetes sepiaria Leaf extract and their catalytic activity to dye degradation. *Materials Science and Eng.* **2017**, 022012 DOI:10.1088/1757-899X/263/2/022012
60. Sartaz, B .; Jenipher, S. A.; Valence, M. K. N.; Baraka L. N. Evaluation of Antibacterial Activities of Tanzanian Moringa oleifera Extracts against Escherichia coli and Klebsiella pneumonia Clinical Isolates. *Tanz. J. of Sci.* **2021**, 47 (3): 1055-1061.
61. Kumar, R. B. Preliminary test of phytochemical screening of crude ethanolic and aqueous extract of Moringa pterygosperma Gaertn. *J. of Pharmacognosy and Photochemistry*, **2015**; 4(1): 07-09.

62. Samuel, J. G. Ch .; Saswati, B.; Selvam, P. E. Optimization of Parameters for Biosynthesis of Silver Nanoparticles Using Leaf Extract of *Aegle marmelos*. *Braz. Arch. Biol. Technol.***2015**, v.58 n.5: pp. 702-710.
63. Thameri. N.A.; Muftin. N.Q.; Al-Rbae. S.H.N. Optimization Properties and Characterization of Green Synthesis of Copper Oxide Nanoparticles Using Aqueous Extract of *Cordia myxa* L. Leaves. *Asian Journal of Chemistry*; **2018**, Vol. 30, No.7 1559-1563.
64. Wageha. A. M.; Ahmed .M. A.R.; Khaled. A.; Elsayed .E. Enhancement of the larvicidal activity of nanostructure copper oxide against *Culex pipiens* mosquito by yttrium replacement based on the crystallite size reduction and topographic surface nature. *Mater. Res. Express* **8**, **2021**. 115006.
65. Radhakrishnan. R.; Liakath.F.A.K.;Muthu. A.; Manokaran .A.; Sundaram.J. S.; Kaviyarasu. K. Green Synthesis of Copper Oxide Nanoparticles Mediated by Aqueous Leaf Extracts of *Leucas aspera* and *Morinda tinctoria*. *Article Letters in applied bio science*.**2021**, Volume 10, Issue 4, 2706 – 2714
66. Muhammad, R. I.; Ebna, J. O.; Saiduzzaman, M .; Shahriyar, S. N.; Debnath,T.; Kabir, A. Effect of Al doping on the structural and optical properties of CuO nanoparticles prepared by solution combustion method: Experiment and DFT investigation. *Journal of Physics and Chemistry of Solids*, **2020**, 109646. DOI:10.1016/j.jpics..109646.
67. Ahid, M.; Al-Fa.; Mahmoud, H.; Abu, K.; and Akl ,M. Green synthesis of copper oxide nanoparticles using *Bougainvillea* leaves aqueous extract and antibacterial activity evaluation. *Chemistry International*.**2021**, 7, 3,155-162.
68. Renugal, D.; Jeyasundari, J.; Shakyhi, A, S. A.; Brightson.Y. A.J. Synthesis and characterization of copper oxide nanoparticles using *Brassica oleracea* var. *italica* extract for its antifungal application. *Mater. Res. Express* .**2020**,7, 045007, 1-6.
69. Sahalie, N. A.; Abrha, L. H.; Tolesa, L. D.; Rakitin, O. *Lamiifolium* (Damakese) as a Treatment for Urinary Tract Infection Chemical Composition and Antimicrobial Activity of Leave Extract of *Ocimum Lamiifolium* (Damakese) as a Treatment for Urinary Tract Infection. *Cogent Chem*. 2018, 4, 1–10.
70. Cieniak, C.; Walshe-Roussel, B.; Liu, R.; Muhammad, A.; Saleem, A.; Haddad, P. S.; Cuerrier, A.; Foster, B. C.; Arnason, J. T. Phytochemical Comparison of the Water and Ethanol

- Leaf Extracts of the Cree Medicinal Plant, *Sarracenia Purpurea* L. (Sarraceniaceae). *J. Pharm. Pharm. Sci.* 2015, 18, 484–493.
71. Suresh, C.M.; Shani, R.; Rohini, T. Biosynthesis of copper oxide nanoparticles using *Enicostemma axillare* (Lam.) leaf extract. *Biochemistry and Biophysics*. www.elsevier.com/locate/bbrep
72. Gnanaprakasam, A.; Sivakumar, V. M.; Thirumarimurugan, M. A Study on Cu and Ag Doped ZnO Nanoparticles for the Photocatalytic Degradation of Brilliant Green Dye: Synthesis and Characterization. *Water Sci. Technol.* 2016, 74, 1426–1435.
73. Masood, A.; Iqbal, T.; Afsheen, S.; Raiz, K.; Nabi, G.; Isan, M.K. Simple synthesis of novel Lanthanum doped Copper oxide nanoparticles for wastewater treatment: A comparison between Experiment and COMSOL simulation. **2022**, pp1-22, DOI: <https://DOI.org/10.21203/rs.3.rs-937180/v1>
74. Rajendaran, K.; Muthuramalingam, R.; Ayyadurai, S. Green Synthesis of Ag-Mo/CuO Nanoparticles Using *Azadirachta Indica* Leaf Extracts to Study Its Solar Photocatalytic and Antimicrobial Activities. *Mater. Sci. Semicond. Process.* **2019**, 9, 230–238.
75. Tsunekawaa.; Fukuda, T. Blue shift in ultraviolet absorption spectra of monodisperse CeO nanoparticles. *Journal of applied physics*, **2000**, volume 87, PP 1318-1321
76. Srivastava, S.; Agarwal, A. Influence of Co doping on structural and optical properties of CuO nanoparticles. *J. of Ovonic Research*, **2018**, Vol. 14, No. 5, p. 395 - 404
77. Alaa, Y.; Ghidana, T.M.A. Akl, A.; Awwad, M. Green synthesis of copper oxide nanoparticles using *Punica granatum* peels extract: Effect on green peach Aphid. *Environmental Nanotechnology, Monitoring, and Management*, **2016**. 6: p. 95-98.
78. Cimen, B.; Sengul, S.; Ergut, M.; Ozer, A. Green Synthesis and Characterization of CuO Nanoparticles: Telon Blue AGLF and Methylene Blue Adsorption. *Sinop Uni J Nat Sci.* **2019**, 4 (1): 1-20.
79. Sivaraj, R.; Pattanathu K.S.M. R.; Rajiv, P.; Abdul, H.S. Biogenic copper oxide nanoparticles synthesis using *Tabernaemontana divaricate* leaf extract and its antibacterial activity against urinary tract pathogen. *Article in Spectrochimica Acta Part A Molecular and Biomolecular Spectroscopy* · May **2014**. DOI: 10.1016/j.saa.2014.05.048.
80. Vanathi.; Prajiv, I.; Sivaraj, R. Synthesis and characterization of *Eichhornia*-mediated copper oxide nanoparticles and assessing their antifungal activity against plant pathogens. *Bull. Mater. Sci.* **2016**, Vol. 39, No. 5, pp. 1165–1170. DOI 10.1007/s12034-016-1276

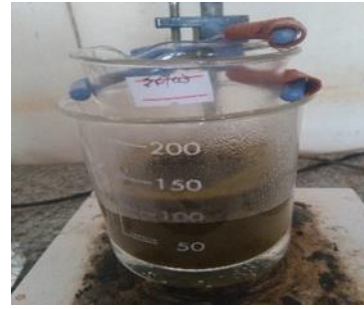
81. Fatima, B.; Siddiqui, Sh.; Ahmed, R.; Ali, S.Ch. Preparation of functionalized CuO nanoparticles using Brassica rapa leave extract for water purification. *Desalination and Water Treatment*, **2019**, pp 192–205.
82. Demirci, D.; Nadaroglu, H.; Alayli, A.G.;4, Nurhan, H. K. Biosynthesis and Characterization of Copper Oxide Nanoparticles using Cimin Grape (*Vitis vinifera* cv.) Extrac. *Int. J. Sec. Metabolite*, **2017**, Vol. 4: 3, pp. 77-84.
83. Menazea, A. A.; Mostafa Figure 15.FTIR analysis of CuO and Co-doped CuO NMs, A. M. Ag Doped CuO Thin Film Prepared via Pulsed Laser Deposition for 4-Nitrophenol Degradation. *J. Environ. Chem. Eng.* **2020**, 8, 104.
84. Ahmad, M. A.; Aslam, S.; Mustafa, F.; Arshad, U. Synergistic Antibacterial Activity of Surfactant Free Ag–GO Nanocomposites. *Sci. Rep.* **2021**, 11, 1–9.
85. Worku, W.A .; Fedlu, K. S.; Endale ,T. M.; Hadgu, H. B.; Bedasa, A. Synthesis of Copper Oxide Nanoparticles Using Plant Leaf Extract of *Catha edulis* and Its Antibacterial Activity. *J. of Nanotechnology. Volume* **2020**, Article ID 2932434.
86. Abdo, E. Z.; Ibrahim, A. I.; Wailed. Study the influence of silver and cobalt on the Photocatalytic activity of copper oxide nanoparticles for the degradation of methyl orange and real wastewater dyes.*Mater.Res.Express*,**7**,**2020** 026201.
87. Batool, M. Studie on Malachite Green Dye Degradation by Biogenic Metal Nano CuO And CuO/ZnO Nano Composites. *Arch. Nanomedicine Open Access J.* **2018**.
88. Elemi, E. E.; Onwudiwe, D. C.; Ogeleka, D. F.; Mbonu, J. I. Phyto-Assisted Preparation of Ag and Ag–CuO Nanoparticles Using Aqueous Extracts of *Mimosa Pigra* and Their Catalytic Activities in the Degradation of Some Common Pollutants. *J. Inorg. Organomet. Polym. Mater.* **2019**, 29, 1798–1806.
89. Soniaa, S.; Jayasudgab, R.; Dhanpal, N. J.; Suresh,P. K.;Mangalaraja,D.;Prabakaran,S. R. Synthesis of hierarchical CuO nanostructures: Biocompatible Antibacterial agents for Gram-positive and Gram-negative bacteria. *Current Applied Physics* **2016**, DOI: 10.1016/j.cap.2016.05.006.
90. Altiketoglu, Melda .; Attar,A.; Erci, F .; Marillena, C. C.; Isildak, I. Green synthesis of copper oxide nanoparticles using *ocimum basilicum* extract and their antibacterial activity. 4 Carol Davila University of Medicine and Pharmacy, **2017**, pp, 7832-7837

91. Bamilaa,R .; Srinivasana, S .;Venkatesanb, A.;Bharath, B .; Perinbamc,K. Structural, optical, and antibacterial activity studies of Ce-doped ZnO nanoparticles prepared by the wet-chemical method. , *Materials Research Innovations*, **2017**,DOI: 10.1080/14328917,1324379.
92. Amiri, M .; Etemadifar, Z.; Daneshkazemi, A .; Nateghi M. Antimicrobial Effect of Copper Oxide Nanoparticles on Some Oral Bacteria and Candida Species. *J Dent Biomater*, 2017;4(1):347-352.

7. APPENDIX

Appendix 1

Copper oxide nanoparticles synthesis



40 mL of Cupric nitrate solution + 20 mL of k.p leaf extract heating at 70 °C for 3 h



Centrifuged



cooled for 20min



Collected on crucible



CuO NMs were formed

Heating on oven

Appendix 2a



Cu(NO₃)₂ solution

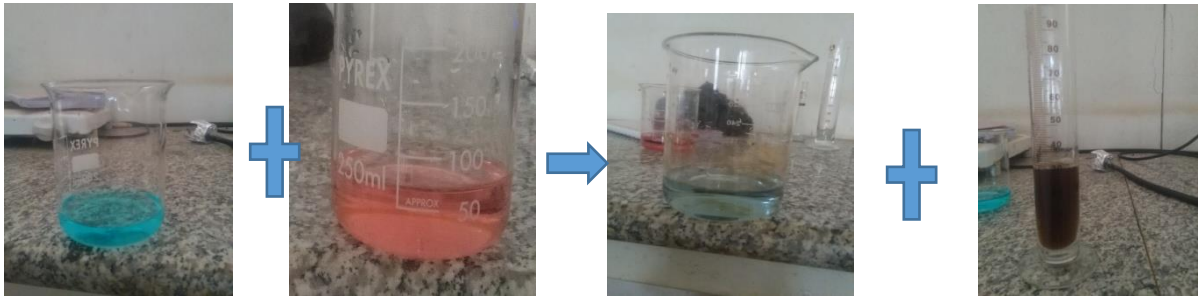


plant extract



CuO NMs

Appendix 2b



A

B

C

D

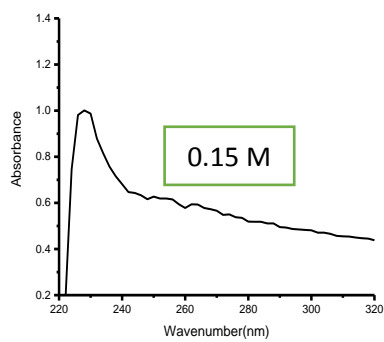
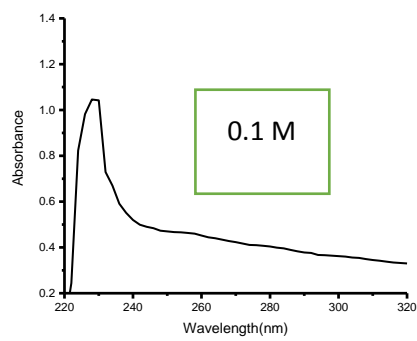
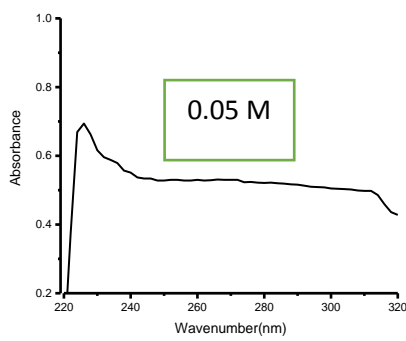


E

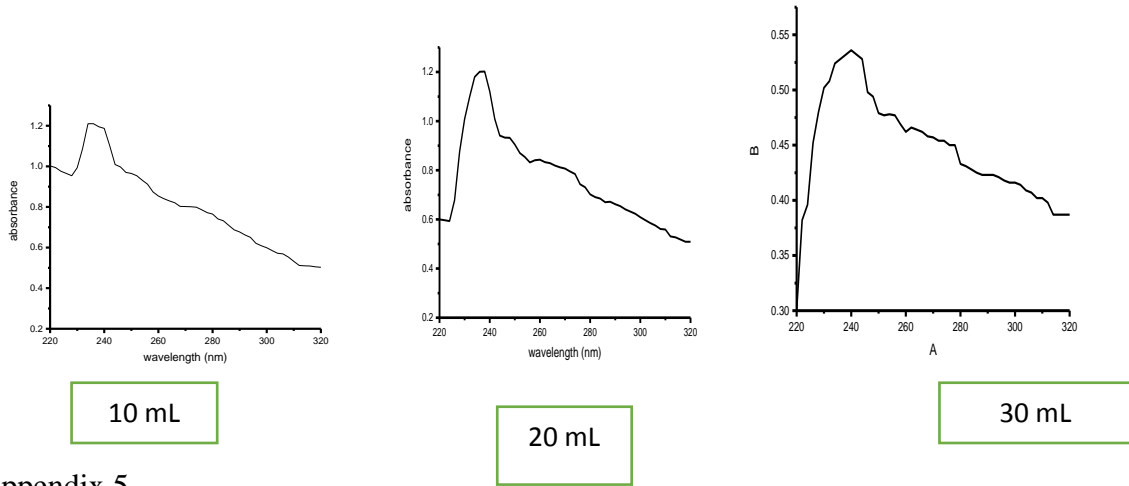
F

A, B, C, D, E, and F indicate copper nitrate solution, cobalt nitrate solution, A+B, plant extract, C+D+NaOH, and Co- doped copper oxide NMs respectively.

Appendix 3



Appendix 4



Appendix 5

